Partial Oxidation of Natural Gas in a Piston Engine: Modeling and Simulation

Diploma Thesis

Hendrik Goßler

Karlsruhe Institute of Technology
Institute for Chemical Technology and Polymer Chemistry

Reviewer: Prof. Dr. Olaf Deutschmann

Duration: November 14, 2013 – May 9, 2014

Erklärung

Hiermit versichere ich, die vorliegende Diplomarbeit selbstständig angefertigt und keine anderen als die von mir angegebenen Quellen und Hilfsmittel verwendet, sowie wörtliche und sinngemäße Zitate als solche gekennzeichnet zu haben. Die Arbeit wurde in gleicher oder ähnlicher Form keiner anderen Prüfungsbehörde zur Erlangung eines akademischen Grades vorgelegt.

Karlsruhe, den 9. Mai 2014

Acknowledgements

Foremost, I would like to thank my supervisor Prof. Olaf Deutschmann for his guidance and for the opportunity to work on this highly interesting topic.

Within the research group, I would like to especially thank Dr. Matthias Hettel for the motivating and fruitful discussions thoughout the whole duration of this thesis. In addition, I thank Dr. Steffen Tischer for the help regarding DETCHEM internals and Dr. Claudia Diehm for the helpful corrections.

I am grateful to my family and friends for their enormous help in structuring and proofreading this thesis.

This thesis was written in the context of the DFG project FOR1993. The financial support for this project is gratefully acknowledged. Finally, I acknowledge the Steinbeis Transferzentrum 240 Reaktive Strömung for making a license to the DETCHEM library available free of cost.

Zusammenfassung

Die Erzeugung von Synthesegas (H_2 und CO) bei gleichzeitiger Gewinnung von mechanischer Energie stellt eine aussichtsreiche neue Anwendungsmöglichkeit von Kolbenmaschinen dar. Aufgrund der großen Anzahl an Kombinationsmöglichkeiten der Betriebsparameter von Kolbenmaschinen, die das Ergebnis der Reaktionen beeinflussen, ist eine Untersuchung der Synthesegasproduktion ausschließlich durch empirische Experimente nicht praktikabel. Eine numerische Untersuchung der Synthesegasproduktion in Kolbenmaschinen ist deshalb unerlässlich.

Zu diesem Zweck wurde in dieser Arbeit ein Computerprogramm namens DETCHEM$^{\text{ENGINE}}$ entwickelt, das die chemische Stoffwandlung im Zylinder einer Kolbenmaschine simuliert. Das zugrundeliegende Modell entspricht einem diskontinuierlich betriebenen Idealreaktor mit zeitlich variablem Volumenprofil. Mit Hilfe dieses Programms wurden basierend auf detaillierten Gasphasenmechanismen zeitaufgelöste Konzentrationsprofile berechnet. Aus diesen wurden Produktzusammensetzung, Ausbeuten und Selektivitäten ermittelt. Das Computerprogramm wurde durch den Vergleich mit zwei anderen Programmen verifiziert. Zunächst wurde das Programm DETCHEM$^{\text{BATCH}}$, ein Teil des Softwarepakets DETCHEM, für einen Vergleich herangezogen. Anschließend wurden Ergebnisse des kommerziell verfügbaren Programms CHEMKIN zur Überprüfung verwendet. Das Modell wurde durch Vergleich mit experimentellen Daten aus der Literatur validiert.

Anhand einer Parameterstudie, die mithilfe von DETCHEM$^{\text{ENGINE}}$ durchgeführt wurde, wurden vielversprechende Betriebsparameter für die Synthesegasproduktion ermittelt. Dabei wurden insbesondere die Produktionsgeschwindigkeiten und Selektivitäten von Wasserstoff und Kohlenstoffmonoxid hinsichtlich des eingesetzten Kraftstoffs untersucht. Interessanterweise zeigten die Simulationen, dass durch das Ersetzen von Stickstoff durch Argon in der Luftkomponente eine 1.5-fache Steigerung der Synthesegasproduktion möglich war. Dies ging ebenfalls mit einer Steigerung des Verhältnisses von H_2 zu CO einher.

Abstract

The simultaneous generation of syngas (H_2 and CO) and power is a promising new application of an internal combustion engine. Due to the abundance of possible combinations of engine operating parameters that influence the outcome of reactions, an analysis of syngas production solely by empirical experiments is impractical. Therefore, it is essential to analyze syngas production in an internal combustion engine numerically.

To this end, a computer program to simulate the chemical conversion inside a cylinder of an internal combustion engine named DETCHEM$^{\text{ENGINE}}$ was developed. The incorporated model corresponds to an idealized batch reactor with a variable volume profile and is based on detailed gas-phase reaction mechanisms. With this program, time-dependent concentration profiles were calculated using detailed gas phase mechanisms. Product compositions, yields and selectivities were derived from these profiles. The computer program was verified by comparing results obtained by two other existing programs. First, a comparison was made against DETCHEM$^{\text{BATCH}}$, a program which is part of the DETCHEM software package. In a second comparison, results from the commercially available CHEMKIN software package were used. The model was validated by comparing results to experimental data described in the literature.

The DETCHEM$^{\text{ENGINE}}$ program was used to conduct a parameter study that identified promising operating conditions for the production of synthesis gas. The study focused on production rates and selectivities of hydrogen and carbon monoxide with respect to the fuel. Interestingly, the simulation showed that substitution of the nitrogen contained in the air component by argon resulted in a 1.5 fold increase of syngas production rate in combination with a higher H_2 to CO ratio.

Contents

Symbols

Symbol	Unit	Description
A	-	symbol of species
A	-	preexponential factor
a	m	crank radius
B	m	bore
b	-	polynomial coefficient
$C_P^\ominus$	J K^{-1} mol^{-1}	standard heat capacity at constant pressure
C_P	J K^{-1} mol^{-1}	molar heat capacity at constant pressure
C_v	J K^{-1} mol^{-1}	molar heat capacity at constant volume
$\bar{c}_v$	J K^{-1}	average heat capacity at constant volume
E_a	J mol^{-1}	activation energy
H	J mol^{-1}	molar enthalpy
$H^\ominus$	J mol^{-1}	standard enthalpy
K	-	equilibrium constant
k	-	rate coefficient
L	m	stroke
l	m	connecting rod length
N	s^{-1}	engine speed
n	mol	amount of substance
$\dot{n}$	mol s^{-1}	reaction rate
N_f	-	number of fuel species
N_r	-	number of reactions
N_s	-	number of species
P	Pa	pressure
q	J	heat
$\dot{q}$	W	heat transfer rate
R	-	ratio of connecting rod length to crank radius
R_0	J K^{-1} mol^{-1}	universal gas constant (8.3144621)
r_c	-	compression ratio
S	J K^{-1} mol^{-1}	entropy
s	m	distance between crank axis and piston
$S^\ominus$	J K^{-1} mol^{-1}	standard entropy
S	-	selectivity

Symbol	Unit	Description
T	K	temperature
U	J mol^{-1}	internal molar energy
u	J	internal energy
V	m^3 mol^{-1}	molar volume
v	m^3	volume
$\dot{v}$	m^3 s^{-1}	derivative of volume w.r.t. time
v_c	m^3	clearance volume
v_d	m^3	displacement/displaced/swept volume
X	-	conversion
x	-	mole fraction
Y	-	yield
Greek Symbols		
α	-	collision efficiency
β	-	temperature exponent
θ	$^\circ$	crank angle
ν	-	stoichiometric coefficient
$\tilde{\nu}$	-	reaction order
τ	s	residence time
ϕ	-	fuel equivalence ratio
$\dot{\omega}$	mol m^{-3} s^{-1}	reaction rate of gas-phase species
Subscripts		
i		species (general)
j		product species
k		reactant species
r		reaction

Acronyms

Acronym	Meaning
AGM	argon gas mixture (20.95 % O_2, 79.05 % Ar)
BC	bottom dead center
CAI	controlled auto ignition
CI	compression ignition
DAE	differential algebraic equation
GRI	Gas Research Institute
HCCI	homogenous charge compression ignition
ICE	internal combustion engine
IDE	integrated development environment
NASA	National Aeronautics and Space Administration
rpm	revolutions per minute
SDA	simplified dry air (20.95 % O_2, 0.93 % Ar 78.12 % N_2)
SI	spark ignition
STR	stirred tank reactor
TC	top dead center
TEL	tetraethyl lead

1. Introduction

1.1. Background and Motivation

Under standard operating conditions, an internal combustion engine (ICE) converts the chemical energy contained in a fuel into mechanical energy. However, even the highest efficiencies barely exceed 50 % [1]. It would be desirable to either increase the efficiency or, in case of stationary applications, to extract additional energy by chemical conversion to useful substances. These substances could be used as starting material for further synthesis while the engine simultaneously generates mechanical energy [2]. In this scenario, exhaust gases would become valuable products.

ICEs are well known for their highly dynamic operation capabilities and are deployed in many different environments. Therefore, current research is aiming at altering the operating conditions of ICEs such that, for example, the fuel (e.g. natural gas) is transformed into higher-grade chemicals. In this context, the engine would effectively become a polygenerator, a device capable of providing more than two forms of energy simultaneously [2] and could be used in synthetic reactions. The principle is to store energy or make it available in a required form, thereby increasing overall efficiency.

An advantage of high-temperature processes as they occur in ICEs is that catalysts are not required. This is especially desirable because catalysts can be very susceptible to degradation, for example by sintering or poisoning [2]. Additionally, catalysts are often expensive noble metals.

1.2. The Internal Combustion Engine

Many types of internal combustion engines exist, varying in size and implementation. Due to their ruggedness, high power to weight ratio and dynamic operation capablities, they have been widely employed in mobile applications such as automotive vehicles, ships and airplanes.

A schematic drawing of a typical engine is shown in Fig. 1.1. A piston is contained in a cylinder and connected to a crankshaft with a connecting rod. This setup allows the reciprocating motion of the piston to be converted into a circular motion in the crankshaft. A fuel-air mixture is introduced into the cylinder and then allowed to react. This results in a pressure rise that pushes the piston downwards, effectively turning the crankshaft. This motion energy can then either be used directly, for example in a vehicle, or be connected to a generator to produce electrical energy.

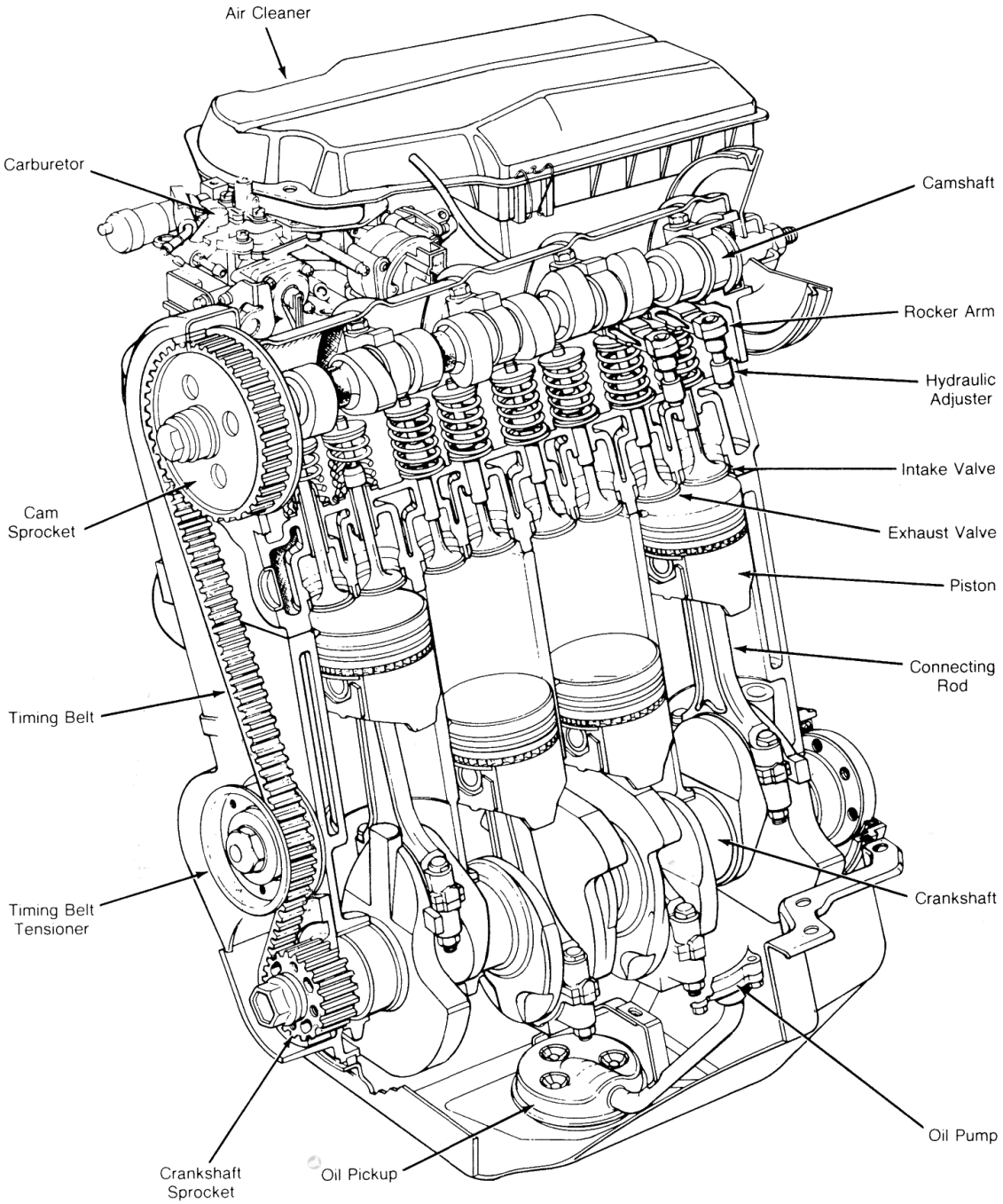

Bore 87.5 mm, stroke 92 mm, compression ratio r_c 8.9, maximum power 65 kW at 5000 rpm

Figure 1.1.: Schematic drawing of a four-cylinder spark-ignition engine (taken from [3]).

It is common to classify them by their method of ignition and by their working cycle. Unless cited otherwise, the information given below is adopted from the textbook "Internal Combustion Engine Fundamentals" by John Heywood [3], from which more details can be obtained. In the following sections, after a brief introduction into the history of the ICE, major types of engines and their modes of ignitions are introduced.

1.2.1. Historical Development

The first internal combustion engine that was a commercial success was developed by J. Lenoir. It dates back to the early 1860s and had a very low efficiency of at most 5 percent. In 1867, N. Otto and E. Langen introduced a more successful engine which reached efficiencies of up to 11 percent. Otto developed the design further and extended the engine cycle to four strokes. The first engine of this kind ran in 1876. At a fundamental level, this engine type is still used today. Therefore, Otto can be considered as the inventor of the combustion engine.

Among the most severe problems encountered was knocking, which is the result of uncontrolled selfignition during the compression phase. Therefore, the maximum possible compression ratio was less than four. These circumstances set an upper limit on the efficiency that could be achieved, since efficiency directly correlates with the compression ratio. Additionally, the four-stroke concept required a complicated engine design.

A new engine type was outlined in a patent by R. Diesel from 1892 that addressed the problem of knocking. He proposed a design in which liquid fuel is injected into the air-filled cylinder during the compression stroke. The mixture then selfignites shortly after the injection solely due to the heat released by the compression of the air. The knock-inhibiting effect of tetraethyl lead (TEL) as a fuel additive in gasoline was discovered at General Motors and became commercially available in 1923. Few years later, E. Houdry discovered a possibility to produce fuels with better antiknock properties. These developments led to a major increase in efficiency, since compression ratios were able to be increased substantially without knocking effects. Furthermore, to simplify engine design, a two-stroke concept was introduced independently by several engineers from Britain and Germany.

Some of these developments were associated with health and environmental problems. As a consequence, laws making requirements to reduce the pollutants were passed and have continuously been enforced. These emission standards had a substantial influence on the further development of engines and combustion technology in general. An interesting review about the usage of TEL in gasoline can be found in [4].

Modern engines are very sophisticated machines and their lines of operation are highly optimized. However, the development was primarily directed towards the efficiency of generating mechanical energy while producing little environmental pollutants and consuming little fuel. Today, the highest possible effiency that can be achieved barely exceeds 50 percent [1].

1.2.2. Methods of Ignition

Probably the most common way to classify an internal combustion engine is to specify how the combustion of the fuel-air mixture is initiated. The combustion process can be initiated either by a spark or by the heat released solely by compression. Since different fuels are used in each case, spark ignition engines are also commonly referred to as gasoline or Otto engines. Compression ignition engines are often called Diesel engines.

Spark Ignition

Spark-ignition (SI) engines possess an electrical spark plug which initiates the combustion process via an electrical discharge between two closely positioned electrodes. A fuel-air mixture is introduced into the cylinder via a carburator or an injection system. The contents of the cylinder is then compressed by the upward piston motion, consequently increasing both pressure and temperature. Before the piston reaches its top most position, the combustion is triggered by a spark. This results in a turbulent flame, which propagates through the combustion chamber until all the fuel has reacted. The pressure then rises rapidly due to the heat released by the reaction. In addition, the hydrocarbons are decomposed to smaller molecules, which further contributes to the pressure rise.

Common problems with this type of engine is the so-called “knock”. Knocking manifests itself as a loud knocking-like noise and is a result of uncontrollable selfignition, i.e. before the electrical spark has ignited the mixture. It is a highly undesirable effect because it is able to cause considerable mechanical damage to the engine components. The damage occurs due to the extremely high pressures that arise from this selfignition at a point where pressure is building up anyways due to the volumetric compression.

Compression Ignition

In a compression-ignition (CI) engine, the cylinder is first filled with air and the compression is started. As a consequence, the temperature increases. Fuel is then injected at a point where the temperature has reached a level above the fuel's ignition point. The most common fuel for this engine type is diesel, a light fuel oil. However, heavier oil fractions are also applicable if they are heated before being injected. Due to their higher weight compared to SI engines, CI engines are more commonly used in medium to large sized applications. Fuel is injected at a similar moment the spark is triggered in an SI engine. The liquid fuel mixes with the hot air and evaporates, effectively creating a reactive fuel-air mixture in some regions of the cylinder volume. Spontaneous ignition occurs after a short delay within these regions and a flame propagates through the parts which have already attained combustable fuel-air ratios. The combustion process along with the now expanding cylinder volume leads to further homogenization of the mixture and allows the rest of the fuel to burn completely. Since the fuel is only introduced into the cylinder when combustion is supposed to proceed, knocking does not occur in CI

engines. However, this engine type is more difficult to build since the higher compression ratios lead to higher pressures and therefore require a sturdier design. It is for this reason that diesel engines are generally heavier than gasoline driven engines.

Homogeneous Charge Compression Ignition

The homogeneous charge compression ignition (HCCI), or also called controlled autoignition (CAI), operating mode can be seen as a hybrid between the SI and the CI types [5]. In a HCCI engine, a homogeneous fuel-air mixture is inducted into the cylinder like in a SI engine. However, the mixture then autoignites as a result of the heat that is generated by the compression, similar to a CI engine. Its advantage compared to the other two types lies in its cleaner and more efficient operation. The trend is clearly going towards using very lean mixtures with equivalance ratios as low as $\phi = 0.2$ [5]. These mixtures have low energy densities leading to lower combustion temperatures, effectively reducing NO_x production. Soot particle production is also reduced because the mixture is homogenized prior to combustion.

It is characteristic for this ignition method that there is no flame propagation as in the SI or CI modes. The mixture rather almost instantaneously ignites in multiple locations in the combustion chamber. The complete combustion heat is released approximately within 5° to 15° crank angle [5]. These very short combustion durations result in a high pressure peak that poses high demands on the mechanical strength of the engine construction. HCCI combustion has several other difficulties, such as weak cold-start capability and the controlling of ignition timing, the latter probably being the most important one [6].

The HCCI effect is not a recent discovery. It has been known since the 1960s [6] and been "rediscovered" in the last decades because of its potential to reduce NO_x emissions and increase efficiency up to the point of diesel engines, even when operated with gasoline. In terms of the fuel used, HCCI engines are very flexible. Reports of even running with wet ethanol exist [7] with the aim of achieving higher net energy efficiency, because significant energy amounts are required to dehydrate ethanol.

From a modeling point of view, the HCCI engine type is easiest to implement. This is because inhomogeneities require substantially more effort to model. Therefore, the HCCI type is of special importance for this work.

1.2.3. Operating Cycles

There are two types of operating cycles: the four-stroke and the two-stroke cycle. In a four-stroke engine, four events occur in sequence to complete a full cycle. For the full cycle to complete, two revolutions of the crankshaft are required. However, only one of these strokes delivers power to the shaft. In two-stroke engines two events comprise a full operating cycle. Therefore, only a single revolution is required for the process to complete. Since there is one power stroke per revolution in the two-stroke engine as

opposed to one power stroke for every two revolutions in the four-stroke engine, two-stroke engines have a higher power-weight ratio than four-stroke engines. Both operation cycles are applicable to SI, CI as well as to HCCI engines. As the four-stroke type is most common and is also implemented in the model, only the individual strokes of this type are described here. The four strokes are:

1. Starting from a piston position at TC, the piston moves downward while the fuel inlet valve is opened until it reaches BC. The cylinder is filled, hence the stroke is called the *intake stroke* or suction stroke.

2. At the beginning of the *compression stroke* the inlet valve is closed. The piston moves from the BC, thus compressing the cylinder contents until it reaches the smallest possible volume (v_c) at TC. Shortly before the piston reaches its topmost position, the combustion is initiated. How it is initiated depends on the engine type.

3. At the beginning of the *power stroke*, pressure and temperature reach their maximum values of the whole operating cycle. The piston is pushed downward by the hot pressurized combustion gases. Work is transferred to the crankshaft via a connecting rod, forcing it to rotate. The stroke is completed once the piston has arrived at the BC.

4. During the *exhaust stroke*, the outlet valve is opened, allowing the combustion products to escape the cylinder via the exhaust as the piston moves upwards. Once the piston has reached the TC, the cycle starts again from the beginning.

1.3. Previous Results Concerning Internal Combustion Engines for Chemical Synthesis

Internal combustion engines have previously not often been the target of research regarding their use for the production of chemicals. Modeling work concerning ICEs has therefore essentially been done to investigate operating characteristics under conventional conditions, i.e. to produce mechanical energy. Very few studies have dealt with their usage as a reactor. In these publications, the production of synthesis gas by partial oxidation, i.e. under fuel-rich conditions, of hydrocarbon fuels was studied. In particular, methane and natural gas as fuels were examined. However, each of the reports lays a focus on a different aspect.

In 1956, von Szeszich studied synthesis gas production in both diesel and gasoline engines with the aim of directly converting heat from chemical reaction to mechanical energy [8]. An important result of this work was that it is possible to operate engines on fuel-rich mixtures of methane and oxygenated air, while simultaneously producing

power. However, he stated that it was difficult to maintain stable operating conditions. For example, highly constant flow rates were essential for this outcome.

Many years later, M. McMillian and S. Lawson carried out both experiments and simulations [9]. In their experiments, they used a spark-ignition engine and laid a focus on particulate emissions. Over the experimental range of equivalence ratios (ϕ) between 1.3 and 1.6, particulate emissions were not higher than when operating the engine with conventional lean mixtures ($\phi = 0.6$). In addition, an HCCI process was modeled and used to study synthesis gas production in the exhaust. Despite the difference of engine type in experiments (SI) and model (HCCI), good agreement between engine data and numerical results was found. Afterwards, the model was used to extend their investigation to fuel-richer mixtures. According to these results, H_2 yields greater than 20 % are possible while still producing mechanical energy.

Subsequently, G. Karim and I. Wierzba further evaluated the operational problems that were reported by von Szeszich [10]. Their experimental setup comprised a dual-fuel compression ignition engine with a compression ratio of 14.2, which more closely approximates an HCCI engine. In order to control ignition timing, the ignition of the premixed methane and air mixture was initiated by the injection of small amounts of diesel. They presented the operating regions constrained by equivalence ratio and oxygen contents in air, in which the mixture either fails to ignite or explosive knocking occurs. They claimed that high levels of syngas (up to 80 % in the dry exhaust) could be produced. Furthermore, carbon formation did not emerge as a problem and the formation of hydrocarbons was not observed.

Next, Yang et al. carried out similar experiments [11]. However, their engine was operated in HCCI mode and had a higher compression ratio ($r_c = 18$). They also presented a map of stable operating regions. However, they varied equivalence ratio and the preheating temperature to reveal regions which were classified as stable, misfire and knocking regions.

Finally, M. Morsy extended the investigation of synthesis gas production in an internal combustion engine on a theoretical basis [12]. In his publication, he pointed out trends regarding variations in equivalence ratio, intake temperature, oxygen enrichment, engine speed, pressure and fuel additives such as H_2O_2 and formaldehyde. By means of a parametric screening study, he determined optimal operating conditions for highest synthesis gas production. However, due to the abundance of combinations of engine operating parameters, only a limited range of parameters was studied.

In conclusion, the research which has been conducted so far represents a number of feasibility studies. The experimental results show that the production of synthesis gas via partial oxidation of methane in the most common engine types is possible. In addition, many of these reports state that the engine was also capable of simultaneously delivering power to the shaft. However, it took some effort to ensure stable engine operation in the experiments.

1.4. Objectives and Approach

The aim of this thesis was to further investigate the possibility to produce chemicals in an internal combustion engine from chemical feedstock such as natural gas. Due to the abundance of possible combinations of engine operating parameters, an investigation carried out solely by experiments is not feasible. Therefore, as a first step this investigation was carried out numerically. To this end, a computer program is needed to describe the chemical conversion inside a cylinder of an ICE. Such a program must output time-dependent concentration profiles from which product compositions, yields and selectivities can be derived.

This is in principle possible with the program DETCHEM$^{\text{BATCH}}$, which is part of the DETCHEM software package. However, parameters specific to ICEs must be preprocessed such that the program can perform the appropriate simulations. This preprocessing step is time consuming and error prone. Conducting a parameter study implies changing these input values repeatedly. Hence, it was desirable to develop a new computer program tailored specifically to the purpose of simulating the chemical process inside an ICE.

The first objective of this thesis was therefore to develop a new computer program. This process should include the conduction of tests in order to eliminate programming errors. Next, the numerical results should be compared with experimental data to evaluate the applicability of the model. Finally, this new program should be used to conduct a parameter study and elucidate syngas production within a range of operating parameters that were not covered in previous studies. In this respect, the focus was laid on selectivities and production rates, as this information is currently not documented in the literature. It was expected that this program can provide further indications as to which operating parameters favor partial oxidation of the fuel instead of full combustion, a situation that reflects conventional operation conditions.

2. Fundamental Definitions and Modeling Approach

The model implemented in the program corresponds to an idealized batch reactor with a variable volume profile. It accounts for the temporal change of species concentrations, volume, temperature and pressure inside the combustion chamber. The combustion chamber is considered to be a single zone without spatial variations in concentration and temperature. Heat loss due to engine cooling is neglected, hence the system operates adiabatically. Only gas-phase reactions are accounted for; surface reactions are not considered.

The simulation begins with a prefilled cylinder with a piston position at BC, equivalent to a crank angle of 180° (see section 2.1.4). A full virtual rotation of the crankshaft is then carried out. First the mixture is compressed (compression stroke). The simulation ends at the end of the power stroke. Only a single cylinder is accounted for and the other two strokes (intake and exhaust) are not considered.

Since a homogeneous mixture is injected into the combustion chamber and selfignites without external influence, the model is expected to be a well-suited approximation of an HCCI engine with a four-stroke operating cycle.

A remark about variable capitalization: A common convention is to denote extensive quantities with variables written in lowercase. Uppercase letters usually denote the corresponding intensive molar quantities. This convention is in conflict with the notation commonly used for volume (V) and pressure (p). In this thesis, the volume and pressure are denoted as v and P in order to strictly adhere to the convention. Accordingly, the molar volume, for example, is denoted by V.

2.1. Governing Equations

A summary of the governing equations of the incorporated model are given below. Their derivations are explained subsequently.

Ideal gas equation:

$$Pv = nR_0T \tag{2.1}$$

Gas-phase species:

$$\frac{\mathrm{d}n_i}{\mathrm{d}t} = v \cdot \dot{\omega}_i \tag{2.2}$$

Temperature:

$$\frac{\mathrm{d}T}{\mathrm{d}t} = \frac{\sum_i (\dot{n}_i \Delta H_i(T) - \dot{n}_i R_0 T) - P\dot{v}}{\bar{c}_v} \tag{2.3}$$

Volume:

$$v = v_\mathrm{c} \cdot \left(1 + \frac{1}{2}(r_\mathrm{c} - 1)\left[R + 1 - \sqrt{R^2 - \sin^2\theta} - \cos\theta\right]\right) \tag{2.4}$$

Crank angle:

$$\theta = 2\pi N \cdot t + \pi \tag{2.5}$$

Derivative of volume with respect to time:

$$\frac{\mathrm{d}v}{\mathrm{d}t} = \frac{1}{2} v_\mathrm{c}(r_\mathrm{c} - 1)\left(\sin\theta + \frac{\sin\theta\cos\theta}{\sqrt{R^2 - \sin^2\theta}}\right)\frac{\mathrm{d}\theta}{\mathrm{d}t} \tag{2.6}$$

Derivative of crank angle with respect to time:

$$\frac{\mathrm{d}\theta}{\mathrm{d}t} = 2\pi \cdot N \tag{2.7}$$

The variables above denote

- P: pressure
- v: volume
- n: species moles
- R_0: universal gas constant
- T: temperature
- $\dot{\omega}$: gas-phase reaction rate
- v_c: clearance volume
- r_c: compression ratio
- R: connecting rod length to crank radius ratio
- θ: crank angle
- N: engine speed

and the index i signifies the species. The residence time of the chemical species in the cylinder corresponds to the total integration time. It is the time required to complete a

full revolution and is determined according to

$$\tau = \frac{1}{N} \,. \tag{2.8}$$

2.1.1. Chemical Kinetics

While thermodynamics determine the equilibrium state of a chemical system, chemical kinetics concern the rate at which chemical reactions proceed [13]. The rate of reaction is defined as the consumption rate of a reactant or the formation rate of a product. Given the general reaction equation

$$\sum_{s}^{N_\mathrm{s}} \nu_s' \mathrm{A}_s \xrightarrow{k} \sum_{s}^{N_\mathrm{s}} \nu_s'' \mathrm{A}_s \,, \tag{2.1}$$

the rate expression of the formation of species i can be formulated as

$$\frac{\mathrm{d}c_i}{\mathrm{d}t} = k(\nu_i' - \nu_i'') \prod_{s}^{N_\mathrm{s}} c_s^{\tilde{\nu}_s'} \,. \tag{2.9}$$

In these equations, A_s denotes the symbol of species s, c_s denotes the concentration of N_s different species s and k is the rate coefficient. The reaction order of the s-th species is denoted by $\tilde{\nu}_s$. Further, ν_i' and ν_i'' are the stoichiometric coefficients of the reactants and products, respectively. Integration of the above equation gives the temporal concentration profile of species i.

It can be seen from Eq. (2.9) that the reaction rate is dependent on the reactant concentrations and on the rate coefficient k. It is characteristic for chemical reactions to exhibit strong temperature dependencies. This temperature dependance of a reaction r is described by the Arrhenius equation

$$k_r = A_r T^{\beta_r} \cdot \exp\left(\frac{-E_{\mathrm{a}r}}{R_0 T}\right) , \tag{2.10}$$

which was empirically formulated. In this equation, E_a denotes the activation energy, A is the preexponential factor, T is the temperature, β is a fitting parameter and R_0 is the universal gas constant. The activation energy corresponds to an energy barrier that the reacting molecules must overcome.

Elementary Reactions and Reaction Mechanisms

Per definition, an elementary reaction proceeds exactly as formulated in the reaction equation on a molecular level [13]. For example, the reaction of hydroxy radicals with

hydrogen

$$\mathrm{OH} + \mathrm{H_2} \longrightarrow \mathrm{H_2O} + \mathrm{H} \qquad \{2.2\}$$

is an elementary reaction. In constrast, the partial oxidation of methane

$$2\,\mathrm{CH_4} + \mathrm{O_2} \longrightarrow 2\,\mathrm{CO} + 4\,\mathrm{H_2} \qquad \{2.3\}$$

is a global (or overall) reaction. This reaction proceeds via many intermediates and does not involve the direct collision of two CH_4 molecules with one molecule of O_2 from which six product molecules emerge. However, the formation and consumption of these intermediates can be described by elementary reactions. Therefore, overall reactions can be described by a sequence of elementary steps. Such a description is called a reaction mechanism. Mechanisms often form a complicated network, whose complexity is a result of the occurance of reversible, parallel and consecutive elementary reactions and a combination of these. It is not uncommon for mechanisms to consist of over 1000 reactions.

The rate of formation of species $\dot{\omega}_i$ is calculated as the sum of all rates of reaction that the species i is involved in (compare Eq. (2.9)):

$$\dot{\omega}_i = \frac{\mathrm{d}c_i}{\mathrm{d}t} = \sum_r^{N_\mathrm{r}} k_r(\nu''_{ri} - \nu'_{ri}) \prod_s^{N_\mathrm{s}} c_s^{\tilde{\nu}'_{rs}} \,. \qquad (2.11)$$

An important characteristic of elementary reactions is that the stoichiometric coefficients of the involved species coincide with the reaction order. Thus, the rate expressions are easily derived. Using $\tilde{\nu}'_{rs} = \nu'_{rs}$, the above equation can be rewritten as

$$\dot{\omega}_i = \sum_r^{N_\mathrm{r}} k_r(\nu''_{ri} - \nu'_{ri}) \prod_s^{N_\mathrm{s}} c_s^{\nu'_{rs}} \,. \qquad (2.12)$$

A strong advantage of detailed mechanisms compared to global rate expressions is that they are valid in a large range of conditions. On the contrary, global rate exressions are fitted to a narrow range of conditions. Therefore, these rate expressions do not allow for a reliable extrapolation to other conditions. This makes the use of reactions mechanisms suitable for the studies within a range of operating parameters that were not covered in experiments, which are the objective of this thesis.

The explicit description of each elementary step comes at the expense of long computational times, since conservation equations of all involved species need to be solved. In most cases, the resulting differential algebraic equation (DAE) system is large and stiff. The stiffness comes from the widely differing time scales of the reaction rates (intermediates such as radicals react rapidly while other species are much more long-lived). Implicit solution methods are used to solve these types of problems. Compared to ex-

plicit methods, the computation of a single integration step is more expensive. However, implicit methods allow for much larger integration step sizes. For the DAEs under consideration, the performance gain by the increased step size outweighs the additional computational effort required for a single step. Hence, implicit solution methods are nearly always used for these types of problems that exhibit a high degree of stiffness.

Relation of Forward and Reverse Reactions

At chemical equilibrium, the rates of the forward and backward reactions are equal. The ratio of the rate coefficients of forward and backward reaction correspond to the equilibrium constant K

$$K = \frac{k_\mathrm{f}}{k_\mathrm{r}} = \prod_s^N c_s^{\nu_s'' - \nu_s'} \,. \tag{2.13}$$

Using

$$K = \exp\left(-\frac{\Delta_\mathrm{r} G^\ominus}{R_0 T}\right), \tag{2.14}$$

the relation

$$\frac{k_\mathrm{f}}{k_\mathrm{r}} = \exp\left(-\frac{\Delta_\mathrm{r} G^\ominus}{R_0 T}\right) \tag{2.15}$$

is obtained. This equation can be rearranged such that the rate coefficient of the reverse reaction can be calculated from thermodynamic data (Eq. (2.34)) and from the rate coefficient of the forward reaction.

The specification of only one direction of a reversible reaction is common practice in published mechanism files. This poses two advantages: firstly, it avoids having to specify redundant data, since the reverse reaction can be calculated from thermodynamic data. Secondly, it ensures that thermodynamic consistency is preserved.

Third Body Reactions

A third particle is often involved in recombination and decomposition reactions [14]. Any species of the mixture can take part in the reaction, therefore a universal species identifier M is introduced:

$$\mathrm{A} + \mathrm{B} + \mathrm{M} \longrightarrow \mathrm{AB} + \mathrm{M} \ \cdot \tag{2.4}$$

Since the efficiency of collisions of different species varies, it is convenient to define an effective concentration of species M by

$$c_{\mathrm{M}} = \sum_i \alpha_i c_i \,. \tag{2.16}$$

Here, α_i is the collision efficiency of the species i with respect to a reference species, for example argon.

Surface Reactions

An important class of reactions are surface reactions, which occur in heterogeneous catalysis. Important characteristics of these are: adsorption of a molecule from the fluid phase onto the surface, reaction of the adsorbed species on the surface and finally the desorption of products. A further description of surface reactions is beyond the scope of this thesis, since only gas phase reactions were considered. However, more information can be found in, for example [13, 15, 16].

2.1.2. Conservation of Energy

Starting point for the derivation of Eq. (2.3) is the first law of thermodynamics

$$\mathrm{d}u = \delta q + \delta w \,, \tag{2.17}$$

which states that the differential change of the internal energy u is equal to the heat q transferred and the work w done to the system [13]. The derivative with respect to time is then

$$\frac{\mathrm{d}u}{\mathrm{d}t} = \dot{q} + \dot{w} \,, \tag{2.18}$$

where $\dot{q}$ is the heat release rate from chemical reaction and $\dot{w}$ is the derivative of the work done to the system with respect to time. The heat of the reaction is given by

$$\delta q = \sum_i -\Delta U_i(T) \cdot \mathrm{d}n_i \,. \tag{2.19}$$

In this equation, n is the mole number of the species i and ΔU is the internal molar energy at temperature T. The minus sign above ensures that a positive value of the heat is obtained if the reaction is exothermal. Since values for the internal molar energies are usually not available, the internal energy needs to be expressed in terms of enthalpies. Using

$$U = H - PV \tag{2.20}$$

where P is the pressure and V is the molar volume, the expression

$$\delta q = \sum_i (\Delta H_i(T) - PV_i) \cdot \mathrm{d}n_i = \sum_i \mathrm{d}n_i \Delta H_i(T) - \mathrm{d}n_i PV_i \tag{2.21}$$

is obtained. To obtain the derivatives with respect to time, the equation is divided by $\mathrm{d}t$:

$$\dot{q} = \sum_i \dot{n}_i \Delta H_i(T) - \dot{n}_i PV_i \,. \tag{2.22}$$

Using the ideal gas law

$$PV_i = R_0 T \,, \tag{2.23}$$

Eq. (2.22) can be rewritten to obtain

$$\dot{q} = \sum_i \dot{n}_i \Delta H_i(T) - \dot{n}_i R_0 T \,. \tag{2.24}$$

The work done to the system is either compression or expansion. Therefore, δw is given as

$$\delta w = -P \,\mathrm{d}v \tag{2.25}$$

and the derivative with respect to time is then

$$\dot{w} = -P\dot{v} \,. \tag{2.26}$$

Equation (2.18) can now be rewritten to

$$\frac{\mathrm{d}u}{\mathrm{d}t} = \sum_i (\dot{n}_i \Delta H_i(T) - \dot{n}_i R_0 T) - P\dot{v} \,. \tag{2.27}$$

The rate of change in temperature is obtained by dividing the above equation by the average heat capacity $\bar{c}_v$

$$\frac{\mathrm{d}T}{\mathrm{d}t} = \frac{\frac{\mathrm{d}u}{\mathrm{d}t}}{\bar{c}_v} \,, \tag{2.28}$$

where

$$\bar{c}_v = \sum_i n_i C_{v,i} = \sum_i n_i (C_{P,i} - R_0) \tag{2.29}$$

and

$$C_v = C_P - R_0 \,. \tag{2.30}$$

This can be rewritten in the form given in Eq. (2.3) in the summary of governing equations. This equation must be solved simultaneously with the species equations.

2.1.3. Calculation of Thermochemical Properties

A common technique to represent the thermochemical properties of a chemical species is by the seven term NASA polynomials. This representation allows the direct calculation of the standard values of heat capacity $C_P^{\ominus}$, enthalpy $H^{\ominus}$ and entropy $S^{\ominus}$ at any temperature, including limited extrapolation beyond the fitted range of the polynomial [17, 18].

A fourth-order polynomial is used to describe the temperature dependance of the heat capacity at standard conditions, for which 5 constants (b_1 to b_5) are required. The remaining 2 (b_6 and b_7) of the 7 coefficients are integration constants for $H_i^{\ominus}(\mathrm{T})$ and $S_i^{\ominus}(\mathrm{T})$. The standard heat capacity $C_{P,i}^{\ominus}(\mathrm{T})$ of a species i is given by

$$C_{P,i}^{\ominus}(T) = R_0 \cdot \left(b_{1,i} + b_{2,i}T + b_{3,i}T^2 + b_{4,i}T^3 + b_{5,i}T^4\right) . \tag{2.31}$$

The enthalpy and entropy are related to $C_P^{\ominus}$ as follows:

$$\begin{aligned} H_i^{\ominus}(T) &= \int C_{P,i}^{\ominus}(T)\,\mathrm{d}T \\ &= R_0\left(b_{1,i}T + \frac{b_{2,i}}{2}T^2 + \frac{b_{3,i}}{3}T^3 + \frac{b_{4,i}}{4}T^4 + \frac{b_{5,i}}{5}T^5 + b_{6,i}\right) \end{aligned} \tag{2.32}$$

$$\begin{aligned} S_i^{\ominus}(T) &= \int \frac{C_{P,i}^{\ominus}(T)}{T}\,\mathrm{d}T \\ &= R_0\left(b_{1,i}\ln T + b_{2,i}T + \frac{b_{3,i}}{2}T^2 + \frac{b_{4,i}}{3}T^3 + \frac{b_{5,i}}{4}T^4 + b_{7,i}\right) . \end{aligned} \tag{2.33}$$

The Gibbs energy can then be calculated via the relation

$$G_i^{\ominus}(T) = H_i^{\ominus}(T) - TS_i^{\ominus}(T) \,. \tag{2.34}$$

In order to achieve higher accuracy, two sets of the 7 constants are provided. One set of coefficients is valid in a low temperature range, while the other set is used for higher temperatures. Thus, a database entry for a single species consists of 14 constants.

2.1.4. Geometrical Parameters of Internal Combustion Engines

The basic geometry including important geometrical parameters is shown in Fig. 2.1. A piston is connected to a crank with radius a via a connecting rod with a length of l. The diameter of the cylinder that the piston is contained in is referred to as the bore B. At a crank angle θ of 0°, the piston is in the top-most position, the top-center (TC). In this position, the volume of the cylinder reaches its minimum and is called the clearance volume (v_c). As the crank is turned, the piston moves downward. The total length it moves until it reaches the lowest possible position is called the stroke (L) and the volume that is swept out during this motion is called the swept or displacement volume (v_d). It is the difference between the total cylinder volume (v_t) and the clearance volume. This position is called the bottom-center (BC) and the crank angle is at 180°.

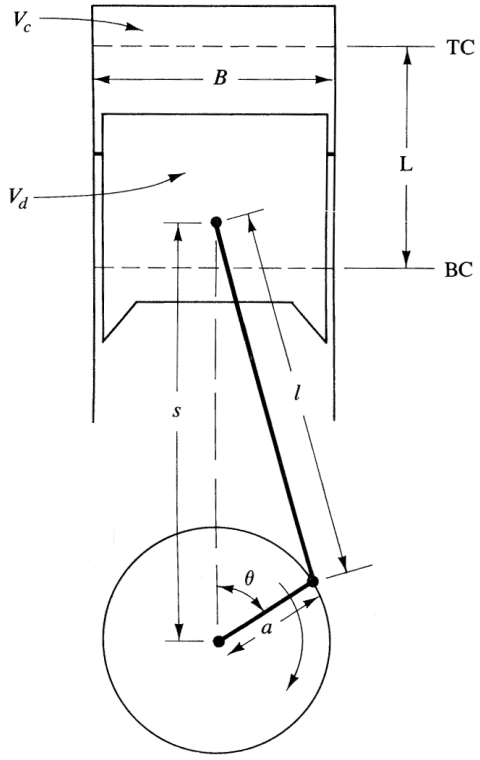

Figure 2.1.: Schematic drawing of the cylinder geometry in an ICE with most important geometrical paramerters (taken from [3]).
Top dead center TC, bottom dead center BC, clearance volume v_c, displacement volume v_d, bore B, stroke L, connecting rod length l, crank radius a, crank angle θ and distance between crank axis and piston s.

The compression ratio r_c is defined as the maximum cylinder volume divided by the minimum cylinder volume. Since maximum volume is equal to the sum of the displacement volume and the clearance volume, it is possible to formulate the compression ratio

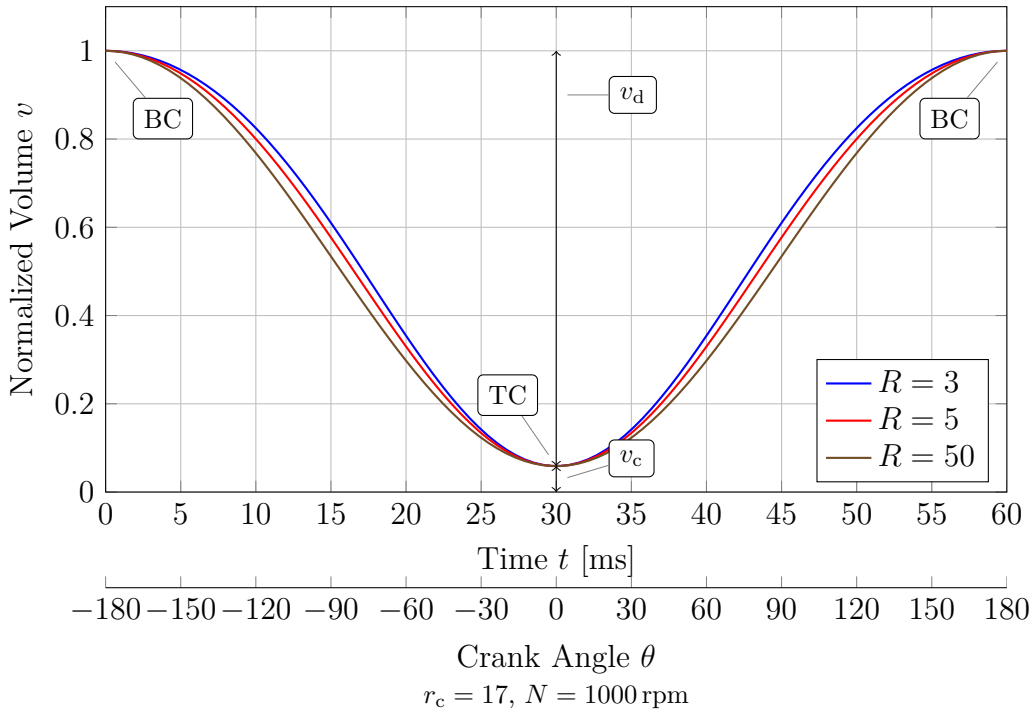

Figure 2.2.: Normalized volume of the combustion chamber as a function of time for three different values of R (ratio of connecting rod length to crank radius).

r_c as follows:

$$r_c = \frac{v_d + v_c}{v_c} \tag{2.35}$$

The values of r_c typically vary from 8 to 12 for SI or from 12 to 24 for CI engines, respectively. Efficiency is directly related to the compression ratio, since more work can be extracted from the process the greater the expansion is.

The volume of the combustion chamber is dependent on the piston position in the cylinder. Hence, the volume is a function of the crank angle θ, which is described by the function

$$v = v_c \cdot \left(1 + \frac{1}{2}(r_c - 1)\left[R + 1 - \sqrt{R^2 - \sin^2\theta} - \cos\theta\right]\right). \tag{2.36}$$

Here, R is the ratio of the length of the connecting rod l to the crank radius a.

$$R = \frac{l}{a} \tag{2.37}$$

Typical values for R range from 3 to 9, depending mainly on engine size. Small engines

tend to have low values (3 to 4), while larger engines typically have larger values (5 to 9). Fig. 2.2 shows the volume with respect to time of a single crankshaft revolution, normalized by the total cylinder volume for 1000 rpm ($16.67\,\mathrm{s}^{-1}$) for different values of R. As can be seen in the figure, the ratio of the length of the connecting rod to the crank radius does not significantly effect the overall shape of the function. Additionally, the following relation exsists between the stroke L and the crank radius a:

$$L = 2a \tag{2.38}$$

In turn, the crank angle is a function of time. The number of revolutions in a given time frame multiplied by 2π is the crank angle in radians. Because the crank angle should be at 180° (BC) for $t = 0$, a correcting term equal to π is introduced:

$$\theta = 2\pi N \cdot t + \pi \tag{2.39}$$

Here, N is the engine speed and t is the time.

2.2. Combustion Stoichiometry and Determination of the Initial Values

For convenience, the computer program is required to handle arbitrary air and fuel compositions that are specified separately. A generally valid procedure for the calculation of the overall mixture composition from the air composition, the fuel composition and the equivalence ratio is outlined in this section. It is assumed that oxygen is the only oxidizing component in the air. Furthermore, only species consisting of carbon, hydrogen, oxygen and sulfur are assumed to take part in the reaction.

The fuel equivalence ratio ϕ is the parameter that uniquely defines the proportions of fuel and air of a mixture and is defined as

$$\phi = \frac{\left(\frac{n_{\mathrm{fuel}}}{n_{\mathrm{O_2}}}\right)}{\left(\frac{n_{\mathrm{fuel}}}{n_{\mathrm{O_2}}}\right)_{\mathrm{stoic}}} \,. \tag{2.40}$$

In this equation, n are the mole numbers. The term denoted by the subscript stoic is the fuel to oxygen ratio required for the stoichiometric combustion according to

$$\mathrm{C}_a\mathrm{H}_b\mathrm{O}_c\mathrm{S}_d + \left(a + \frac{b}{4} - \frac{c}{2} + d\right)\mathrm{O_2} \longrightarrow a\,\mathrm{CO_2} + \frac{b}{2}\,\mathrm{H_2O} + d\,\mathrm{SO_2} \;\cdot \tag{2.5}$$

Based on this generalized reaction equation, the expression

$$\left(\frac{n_{\text{fuel}}}{n_{\text{O}_2}}\right)_{\text{stoic}} = \left[n_{\text{C}} + \frac{1}{4}n_{\text{H}} - \frac{1}{2}n_{\text{O}} + n_{\text{S}}\right]^{-1} \tag{2.41}$$

can be formulated by comparing the coefficients. Here, the n on the right-hand side is the atomic composition of the fuel molecule, e.g. $n_{\text{H}} = 4$ for CH_4. To accomodate for fuel mixtures, the expression becomes

$$\left(\frac{n_{\text{fuel}}}{n_{\text{O}_2}}\right)_{\text{stoic}} = \left[\sum_i^{N_\text{f}} x_i \left(n_{\text{C},i} + \frac{1}{4}n_{\text{H},i} - \frac{1}{2}n_{\text{O},i} + n_{\text{S},i}\right)\right]^{-1}, \tag{2.42}$$

where N_f is the number of fuel species and x_i is the mole fraction of species i in the fuel component. Combining Eq. (2.40) and (2.42) leads to

$$\left[\sum_i^{N_\text{f}} x_i \left(n_{\text{C},i} + \frac{1}{4}n_{\text{H},i} - \frac{1}{2}n_{\text{O},i} + n_{\text{S},i}\right)\right]^{-1} \phi = \left(\frac{n_{\text{fuel}}}{n_{\text{O}_2}}\right). \tag{2.43}$$

So far, it has not been accounted for that the oxidizing component (usually air) can also be a mixture. To this end, the mole number of oxygen in the above equation needs to be expressed in relation to the air. Using

$$n_{\text{O}_2} = n_{\text{air}} \cdot x_{\text{O}_2,\text{air}}\,, \tag{2.44}$$

where $x_{\text{O}_2,\text{air}}$ is the mole fraction of O_2 in the air component, Eq. (2.43) then becomes

$$\left[\sum_i^{N_\text{f}} x_i \left(n_{\text{C},i} + \frac{1}{4}n_{\text{H},i} - \frac{1}{2}n_{\text{O},i} + n_{\text{S},i}\right)\right]^{-1} \phi \cdot x_{\text{O}_2,\text{air}} = \frac{n_{\text{fuel}}}{n_{\text{air}}} = \frac{x_{\text{fuel}}}{x_{\text{air}}}\,. \tag{2.45}$$

By using

$$x_{\text{fuel}} + x_{\text{O}_2} = 1\,, \tag{2.46}$$

the equation can be rewritten to the desired forms:

$$x_{\text{fuel}} = \frac{\left[\sum_i^{N_\text{f}} x_i \left(n_{\text{C},i} + \frac{1}{4}n_{\text{H},i} - \frac{1}{2}n_{\text{O},i} + n_{\text{S},i}\right)\right]^{-1} \phi \cdot x_{\text{O}_2,\text{air}}}{1 + \left[\sum_i^{N_\text{f}} x_i \left(n_{\text{C},i} + \frac{1}{4}n_{\text{H},i} - \frac{1}{2}n_{\text{O},i} + n_{\text{S},i}\right)\right]^{-1} \phi \cdot x_{\text{O}_2,\text{air}}}\,, \tag{2.47}$$

$$x_{\text{air}} = \frac{1}{1 + \left[\sum_i^{N_\text{f}} x_i \left(n_{\text{C},i} + \frac{1}{4}n_{\text{H},i} - \frac{1}{2}n_{\text{O},i} + n_{\text{S},i}\right)\right]^{-1} \phi \cdot x_{\text{O}_2,\text{air}}}\,. \tag{2.48}$$

Calculation of the Initial Values

To determine the initial values, the total number of moles in the system must be calculated. Since ideal gas behavior is assumed, the total number of moles is given by

$$n = \frac{Pv}{R_0 T}\,. \tag{2.49}$$

The initial volume (at BC) is known from the engine geometry. Therefore, the user must provide the two remaining variables: intake temperature T and initial pressure P. With Eq.(2.47) and (2.48), the calculation of the moles of each species is now straight-forward. The total moles n multiplied by each species mole fraction x_i yields the moles n_i of the respective species:

$$n_i = n \cdot x_i \tag{2.50}$$

2.3. Calculation of Selectivity, Yield, Conversion and Production Rate

To calculate the selectivities S, the relation

$$S_{j,k} = \frac{Y_{j,k}}{X_k} \tag{2.51}$$

was used. Here, Y is the yield of species j with respect to reactant k and X is the conversion. The yield is calculated as

$$Y_{j,k} = \frac{n_j^{\text{in}} - n_j^{\text{out}}}{n_k^{\text{in}}} \frac{\nu_k}{\nu_j} \tag{2.52}$$

(ν: stoichiometric coefficient) and the conversion of the reactant species k as

$$X_k = \frac{n_k^{\text{in}} - n_k^{\text{out}}}{n_k^{\text{in}}}\,. \tag{2.53}$$

With the above definitions for Y and X, Eq. (2.51) can be rewritten to

$$S_{j,k} = \frac{n_j^{\text{in}} - n_j^{\text{out}}}{n_k^{\text{in}} - n_k^{\text{out}}} \frac{\nu_k}{\nu_j}\,. \tag{2.54}$$

In this thesis, the calculations should be performed with respect to many reactants, since the fuel was a mix of hydrocarbons. In this case, it is convenient to perform the calculations element-wise. Then the fraction of stoichiometric coefficients above becomes

minus unity.
For H_2:

$$S_{H_2,\text{fuel}} = \frac{n^{\text{out}}_{\text{H},H_2} - n^{\text{in}}_{\text{H},H_2}}{n^{\text{in}}_{\text{H,fuel}} - n^{\text{out}}_{\text{H,fuel}}} \tag{2.55}$$

For H_2O:

$$S_{H_2O,\text{fuel}} = \frac{n^{\text{out}}_{\text{H},H_2O} - n^{\text{in}}_{\text{H},H_2O}}{n^{\text{in}}_{\text{H,fuel}} - n^{\text{out}}_{\text{H,fuel}}} \tag{2.56}$$

For CO:

$$S_{\text{CO,fuel}} = \frac{n^{\text{out}}_{\text{C,CO}} - n^{\text{in}}_{\text{C,CO}}}{n^{\text{in}}_{\text{C,fuel}} - n^{\text{out}}_{\text{C,fuel}}} \tag{2.57}$$

For CO_2:

$$S_{CO_2,\text{fuel}} = \frac{n^{\text{out}}_{\text{C},CO_2} - n^{\text{in}}_{\text{C},CO_2}}{n^{\text{in}}_{\text{C,fuel}} - n^{\text{out}}_{\text{C,fuel}}} \tag{2.58}$$

The production rate (unit: mol s^{-1}) is calculated by the equation

$$\dot{n}_i = \frac{N}{2} n_i \,, \tag{2.59}$$

where N is the engine speed and n is the amount of substance in the exhaust of species i. Two revolutions are required to complete the full cycle in a four-stroke engine. Therefore, the engine speed must be divided by 2.

3. Development and Verification of the Computer Program

In the context of this thesis, a new computer program named DETCHEM$^{\text{ENGINE}}$ was developed to facilitate the simulation of homogeneous gas-phase reactions in an internal combustion engine. The compression and expansion strokes are mimicked by a time-dependent volume profile, which is derived from geometrical parameters of the engine. The program is built on top of the DETCHEM library (version 2.4) and uses the LIMEX solver. It is possible to provide compositions of the air and the fuel, the equivalence ratio and various engine geometry parameters. The program outputs temporally resolved profiles of moles, temperature, volume and pressure in text format, which can be easily imported to spreadsheet software for data analysis.

First, the development of the program is outlined, explaining the file and program structure. Subsequently, tests comparing DETCHEM$^{\text{ENGINE}}$ with established simulation tools were carried out for verification purposes.

3.1. Software Involved in the Development

DETCHEM consists of several programs (or models) and library modules [14]. The core of the DETCHEM package is represented by the `lib_detchem` library, which is a collection of subroutines for the calculation of reaction rates, species transport and thermochemical properties. Furthermore, the `lib_input` library provides functionality to read input files supplied by the user, including elementary step reaction mechanisms. A detailed description of the formats of these files can be found in the DETCHEM manual [14].

DETCHEM$^{\text{ENGINE}}$ makes use of the following functionality provided by the DETCHEM libraries: Firstly, the reading of the various input files is done by `lib_input`. These are the thermodynamic data file in the NASA polynomial form, the mechanism file and the program specific settings file, the latter two being in the DETCHEM format. Furthermore, the ENGINE code resorts to DETCHEM subroutines to calculate enthalpies (Eq. (2.3)), molar heat capacities (Eq. (2.29)) and reaction rates (Eq. (2.2)). Additionally, the DETCHEM$^{\text{BATCH}}$ program was used as a reference to guide the development process.

In order to calculate temporal profiles of concentrations, the DAE system given by Eq. (2.2) and Eq. (2.3) must be solved. For this purpose, LIMEX (version 4.2A1) is used, which is an integrator written in `Fortran` that employs an implicit solution method [19].

Further software involved in the development of DETCHEM$^{\text{ENGINE}}$ was `make`, which is a

build tool, and GDB, which was used for debugging. In addition, Git was used as a version control system. The Netbeans IDE (integrated development environment) was chosen to develop the computer program because it features Fortran syntax highlighting, integration with Git and most importantly debugging capabilities with GDB. Finally, scripts written in Python were developed to facilitate data analysis and evaluation. Their usage is described in the manual in Appendix A.

3.2. The Build Process and File Structure

The first step in developing the computer program was to modify the file structure and build process of the DETCHEM package as to make the debugging process easier and faster. In order to use debugging tools such as GDB, it is necessary to compile the program using special compiler flags. However, a program compiled with these flags set (debug mode) will run significantly slower than when compiled without. It is therefore desirable to be able to easily switch between different compile types (also: build types).

In the modified build process, two compile types can be specified via an additional argument to the build command: a release type and a debug type. This approach has the advantage that making changes to make's configuration file (the makefile) is not necessary when switching between compile types. Furthermore, all object files resulting from the compilation are stored in separate locations for each compile type. This separation avoids having to recompile the whole program including all libraries, when changing compile types. More detailed usage information can be found in Appendix A.

An excerpt of the directory contents is given below. Directories are denoted by an appended slash (/).

```
bin/
  debug/
    engine          <- the executable, compiled with debug flags set
  release/
build/              <- contains object files created by the compiler
  debug/
    lib/
    modules/        <- contains module files created by the compiler
    src/
      engine/
        config.o
        ...
  release/
lib/                <- contains source code of the libraries
  detchem/
  limex/
src/                <- contains source code of the program
  engine/
    config.f95
    main.f95
```

```
    output.f95
    physical_constants.f95
    solver.f95
tools/              <- contains the python scripts
  configure.py
  mole_fractions_exhaust.py
  moles_exhaust.py
```

The `src/` directory contains all the source code files of the program. Those of the libraries can be found in `lib/`. In the new build process, binary files are created within `bin/` in a subdirectory corresponding to the build type, i.e. `debug/` and `release/`. Object and module files of the program and the libraries are created within subdirectories of the `build/` directory. The structure of these subdirectories reflects that of the directories containing the source code (`src/` and `lib/`). Finally, the `Python` scripts are located in `tools/`.

3.3. Program Structure

DETCHEM$^{\text{ENGINE}}$ is structured in `Fortran` modules, which contain all of the program logic. The `main.f95` file contains the main program, whose only purpose is to initialize the modules in the appropriate order. This approach allows for a clear program layout.

Four modules are defined, of which each is responsible for performing a specific task. Every module defines an `init` subroutine, which serves to setup the module. A further explantation of the modules is given below.

`engine_config` The purpose of this module is to validate and import user data, which is then provided to the other modules. As with all `DETCHEM` programs, the user specifies the various available settings via an input file in text format. Additionally, the mechanism and the thermodynamic data are provided in the form of input files. When the `engine_config` module is initialized, these input files are read by calling subroutines from the `lib_input` library. The contents of the files are transferred into an internal data structure for use by the other modules. Furthermore, user input is validated and in case of faulty values, the program aborts. Finally, the total mole fractions from a given air composition, fuel composition and equivalence ratio are calculated.

`engine_output` This module's `init` subroutine prepares the output file `result.plt`, to which the simulation results are written. Additionally, the module provides a `write_data` subroutine that writes the time, pressure, volume, temperature and mole numbers of all species defined in the mechanism to the `result.plt` file. Internally, it calls routines from the `DETCHEM` library.

`engine_solver` This module represents the core of the `ENGINE` program. The `init` subroutine configures the `LIMEX` solver according to the user input, which is accessed via the `engine_config` module. This includes the calculation of the initial values of the DAE. Additionally, the `engine_output` module is initialized. Furthermore, the `engine_solver` module defines a subroutine `solve_DAE_system`, which integrates the DAE system. This subroutine is called from the main program after all modules have been initialized. During the integration, the `write_data` routine is called at fixed intervals.

`physical_constants` This module does not contain any program logic. Only the required physical constants are defined.

3.4. Verification of the Computer Program

The purpose of the following verification was to eliminate programing errors. To this end, comparisons with well established simulation tools are a suitable measure. An essential requirement of these reference tools is that the underlying chemical model closely resembles the one incorporated in the program to be tested. A second requirement is that all programs involed in the comparison must be configurable in such a way, that the simulation conditions are equivalent for each case.

The program developed in this thesis is compared to `DETCHEM`$^{\texttt{BATCH}}$ and to the `CHEMKIN` (version 3.7.1) application. Simulation results from the `BATCH` code were obtained by directly executing the program. This was not possible with `CHEMKIN` because it is commercial software and no copy was at hand. Instead, the results were obtained from a recently published parameter study which was conducted by said version of `CHEMKIN`. In order to extract the data from the graphical figures from the article, the application `GraphClick` was used.

3.4.1. Comparison with DETCHEM$^{\text{BATCH}}$

The `DETCHEM` software package includes a program named `DETCHEM`$^{\texttt{BATCH}}$ [14]. It is a simulation tool for both gas-phase and surface reactions in an idealized batch reactor (or stirred tank reactor, STR). The model assumes perfect mixing, hence there are no spatial gradients with respect to concentration and temperature within the reaction vessel. The available configuration options relevant for the purpose of this comparison are: the mode of operation (adiabatic or isenthalpic), integration time and the initial mole fractions. Further, it is possible to specify a time-dependent volume profile as key-value pairs.

The `BATCH` code has been thoroughly tested and shown to work reliably [14]. Within the scope of this comparison, it is therefore considered as a benchmark. Because the

underlying chemical model of both programs is identical, results of both the ENGINE and the BATCH code must be identical when run with corresponding settings.

Compared to DETCHEM$^{\text{ENGINE}}$, DETCHEM$^{\text{BATCH}}$ has a much richer feature set and is therefore a more general tool for solving STR-type problems. For example, sensitivity and reaction flow analysis are not possible with the ENGINE code. However, since DETCHEM$^{\text{ENGINE}}$ is tailored specifically to solving problems regarding internal combustion engines, its advantage lies in its much more convenient usage. Parameters specific to the internal combustion engines (compression ratio, clearance volume, etc.) can be directly specified in DETCHEM$^{\text{ENGINE}}$.

Equivalent settings with the following parameters were set in both programs: an equivalence ratio of 2.5, an engine speed of 1000 rpm, an intake temperature of 500 K (227 °C) and an initial pressure of 1.0 bar. The geometry of the simulated engine is shown in Table 4.2 on page 34. The volume profile used in the BATCH simulation was calculated by the DETCHEM$^{\text{ENGINE}}$ program. The input files of both programs are given in Appendix B.

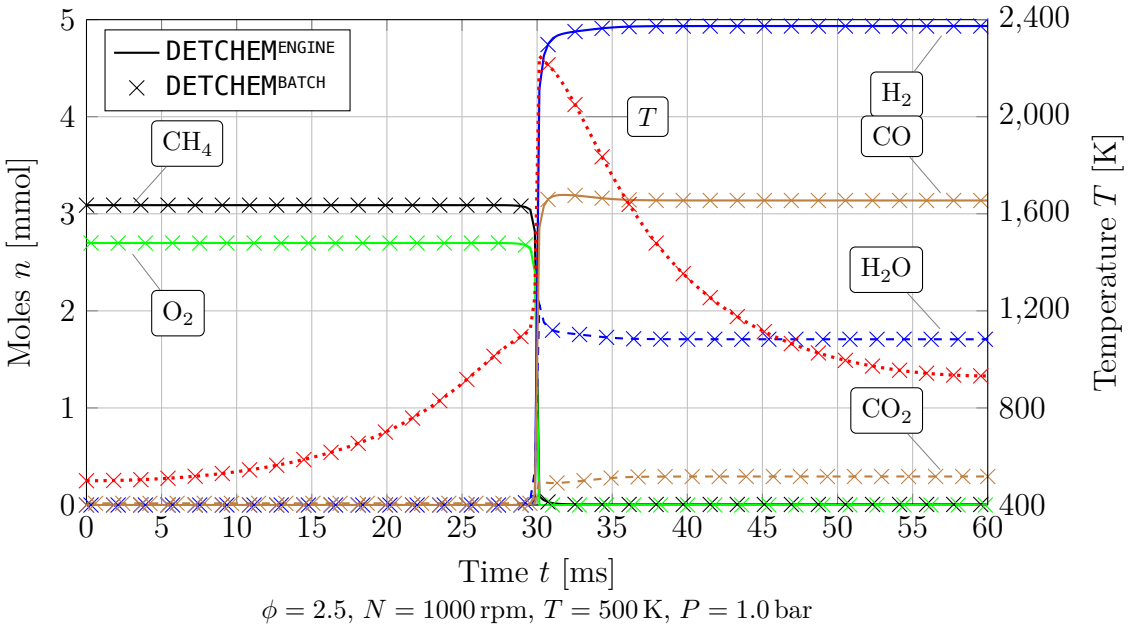

Figure 3.1.: Reaction progress showing moles and temperature as a function of time for both DETCHEM$^{\text{ENGINE}}$ and DETCHEM$^{\text{BATCH}}$. The lines represent the results obtained from ENGINE, the symbols denote values from BATCH.

Fig. 3.1 shows the temporal profiles of the moles and of temperature. A plot comparing the data obtained with DETCHEM$^{\text{ENGINE}}$ and DETCHEM$^{\text{BATCH}}$ is shown in this figure. Lines represent the results obtained from ENGINE and the symbols denote values from BATCH. The diagram clearly shows that both programs produce nearly identical results, thus confirming that the chemical model is correctly implemented in DETCHEM$^{\text{ENGINE}}$. Small

deviations in the order of 10^{-7} to 10^{-17} in the exhaust mole numbers exist. They are not visible in the figure because of the chosen scale of the y-axis.

Performance

In course of the verification of the DETCHEM$^{\text{ENGINE}}$ program, it became apparent that the ENGINE comes to the same results significantly faster than the BATCH code. Further investigations confirming this are summarized in Table 3.1. All calculations were conducted on a machine with an Intel Core i7-3930K Processor running at 3.2 GHz and with 12 GB RAM. Three consecutive runs with the same configuration (as above) were carried out with both programs. While DETCHEM$^{\text{ENGINE}}$ was able to finish the simulations in an average of 9 min 48 s, DETCHEM$^{\text{BATCH}}$ took an average of 3 h 34 min 35 s to complete. This corresponds to a factor of 21.9.

	run 1	run 2	run 3	average
ENGINE	9 min 49 s	9 min 49 s	9 min 47 s	9 min 48 s
BATCH	3 h 34 min 33 s	3 h 34 min 29 s	3 h 34 min 42 s	3 h 34 min 35 s

$\phi = 2.5$, $N = 1000\,\text{rpm}$, $T = 500\,\text{K}$, $P = 1.0\,\text{bar}$

Table 3.1.: Execution times of DETCHEM$^{\text{ENGINE}}$ and DETCHEM$^{\text{BATCH}}$. The ENGINE progam completed the simulation with the above settings 21.9 times faster than the BATCH program.

3.4.2. Comparison with CHEMKIN

CHEMKIN is a software package used to simulate chemical processes in a variety of applications. It is commercial software and a very frequently used simulation tool in chemistry applications.

In a recent publication from 2014, M. H. Morsy conducted a comprehensive parameter study to investigate the possibility to produce synthesis gas in an internal combustion engine [12]. In this study, only modeling results were presented. The simulations were performed by using the closed homogeneous reactor model from the CHEMKIN software package. In contrast to the model implemented in DETCHEM$^{\text{ENGINE}}$, the CHEMKIN model accounts for the heat exchange between the gas and cylinder walls [12]. Heat loss is considered by employing the heat transfer correlation published by G. Woschni that takes the convective terms from both the piston motion and the combustion into account [20].

Apart from this, the models and the boundary conditions are the same. Therefore, the use of the results from this article as a reference to verify the program presented in this thesis is warranted.

For the simulations in the reference article, all engine components were assumed to be at a constant temperature of 450 K (177 °C). The geometry of the simulated engine can be taken from Table 4.2 (page 4.2). Since there was no indication of the air composition used in the reference article, it was assumed to be dry air as described in section 4.1 and shown in Table 4.1. Unless specifically stated otherwise, the initial pressure was assumed to be 1.0 bar.

For the purpose of this verification, data points of four figures from Morsy's publication were extracted and used as a reference [12]. Since all four data sets showed excellent agreement, further data sets were not examined. In all figures in this section, the results from both programs are plotted. The triangles represent simulation results obtained with DETCHEM$^{\text{ENGINE}}$, while the circles denote values from the reference document. The normalization of Fig. 3.4 and 3.5 was done by mole fractions of the fuel components at the inlet ($t = 0$).

Fig. 3.2 shows the H_2 to CO ratio as a function of equivalence ratio while keeping all other parameters constant. Overall, near-exact concordance between the two result sets was found. The greatest deviation of 0.4 % is between the last two data points ($\phi = 3.5$).

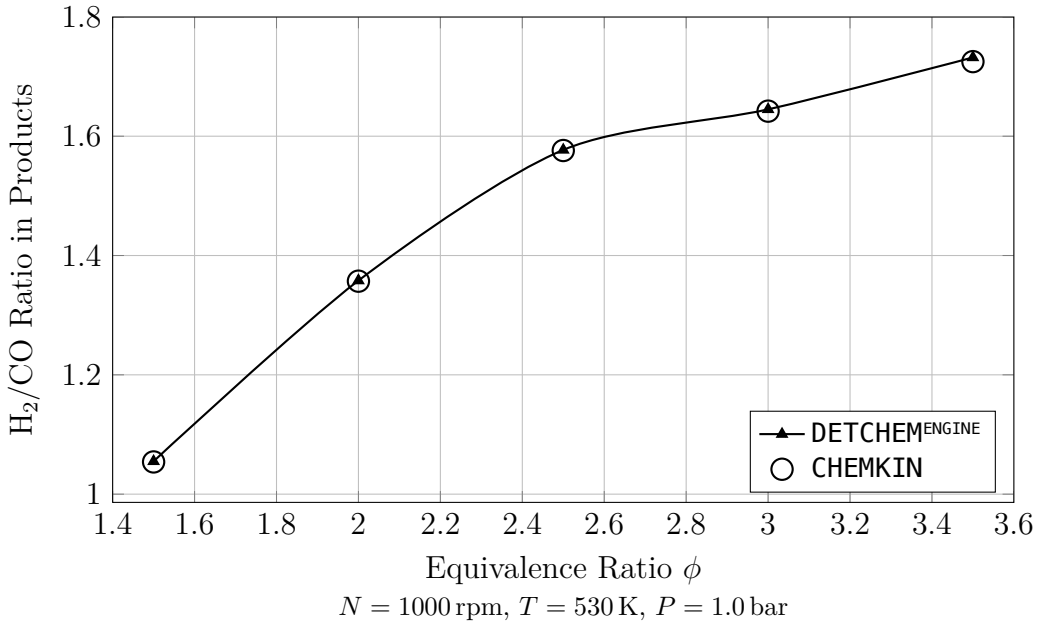

Figure 3.2.: Effect of equivalence ratio on the H_2/CO ratio in the combustion products, showing excellent agreement between DETCHEM$^{\text{ENGINE}}$ and CHEMKIN results (adopted from [12], Fig. 2). The triangles represent results obtained from ENGINE, the circles denote values from CHEMKIN.

Fig. 3.3 shows the mole fractions of H_2 and synthesis gas as a function of equivalence ratio for three different engine speeds (500 rpm, 1000 rpm and 1500 rpm). Again, excel-

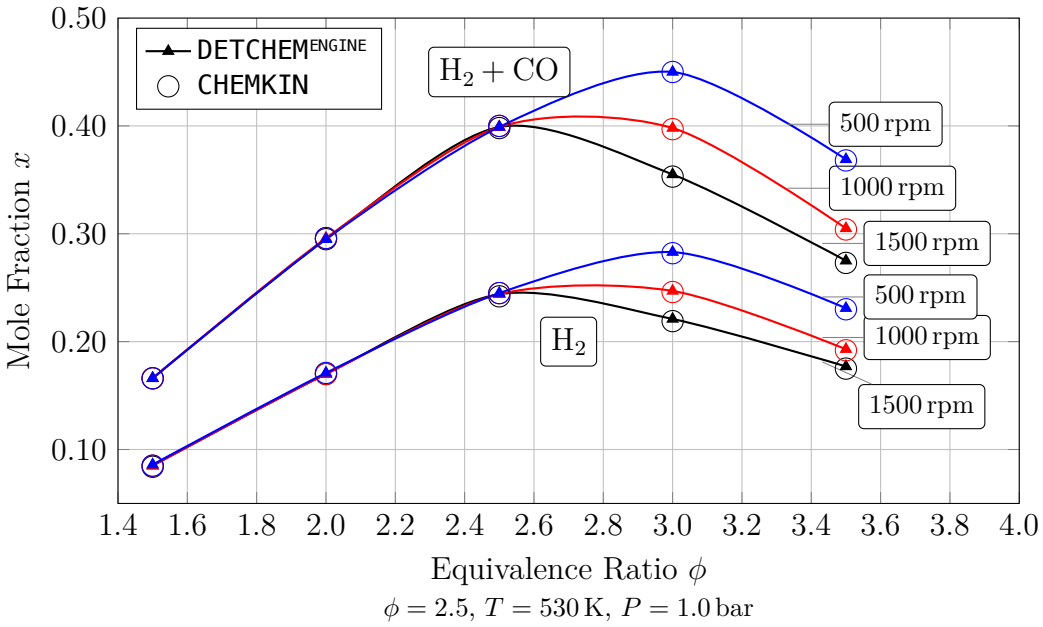

Figure 3.3.: Effect of equivalence ratio on the exhaust mole fractions of H_2 and syngas for three different engine speeds, showing excellent agreement between DETCHEM$^{\text{ENGINE}}$ and CHEMKIN results (adopted from [12], Fig. 5). The triangles represent results obtained from ENGINE, the circles denote values from CHEMKIN.

lent agreement between the CHEMKIN results and those obtained with DETCHEM$^{\text{ENGINE}}$ was found.

In order to investigate the effect of intake temperature (or preheating temperature), Morsy conducted several simulations at varying temperatures and for two equivalence ratios (2.5 and 3.5). Fig. 3.4 shows the results obtained by both DETCHEM$^{\text{ENGINE}}$ and CHEMKIN. The DETCHEM results are in near perfect agreement to the CHEMKIN results. In addition, the author states that for $\phi = 2.5$ autoignition did not occur below 465 K (490 K for $\phi = 3.5$, 192 °C and 217 °C respectively). This could also be confirmed.

Reproduction of the results shown in Fig. 3.5 was again possible with excellent agreement. The figure shows the effect of initial pressure on the mole fractions of synthesis gas. All simulations were carried out with an engine speed of 1000 rpm, an equivalence ratio of 2.5 and at three different intake temperatures (470 K, 480 K and 500 K).

3.4.3. Conclusion

It could be shown that the computer program developed in this thesis is capable of producing accurate results when compared to widely used commercially available software. All results obtained with DETCHEM$^{\text{ENGINE}}$ were in excellent concordance to those generated

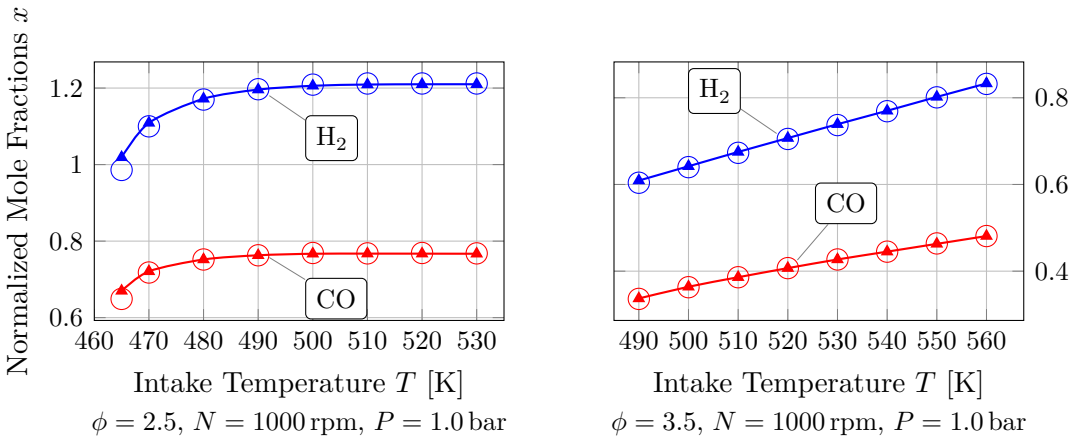

Figure 3.4.: Effect of intake temperature on syngas production, showing excellent agreement between DETCHEM$^{\text{ENGINE}}$ and CHEMKIN results (adopted from [12], Fig. 3). The triangles represent results obtained from ENGINE, the circles denote values from CHEMKIN.

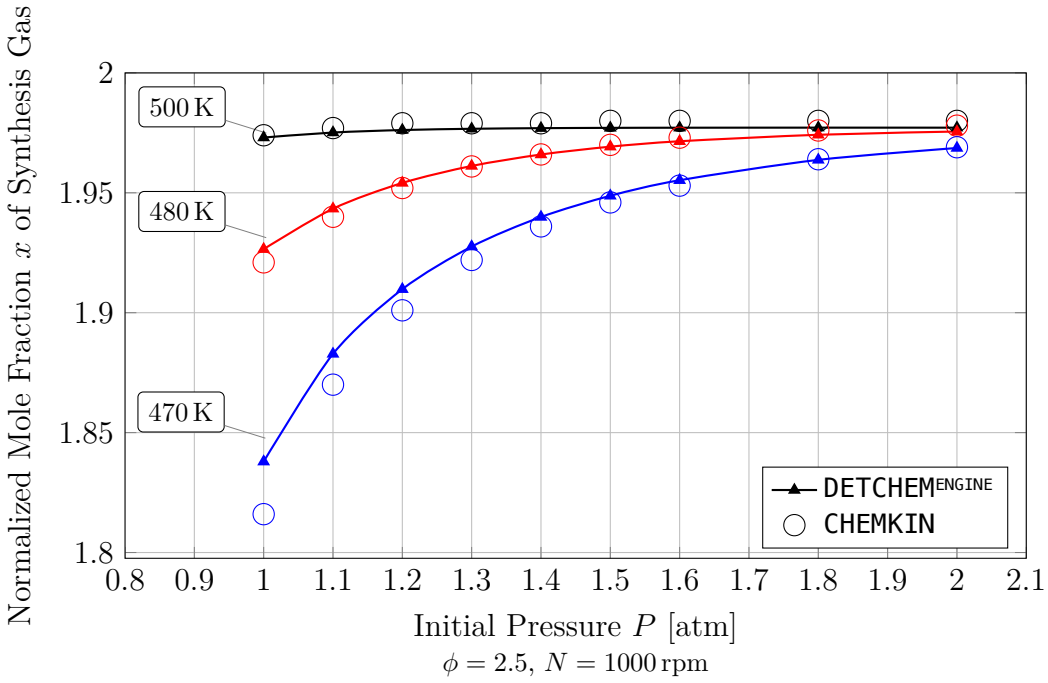

Figure 3.5.: Effect of initial pressure on the production of synthesis gas for three different intake temperatures, showing excellent agreement between DETCHEM$^{\text{ENGINE}}$ and CHEMKIN results (adopted from [12], Fig. 9). The triangles represent results obtained from ENGINE, the circles denote values from CHEMKIN.

with either DETCHEM^{BATCH} or CHEMKIN. Surprisingly, the agreement between the ENGINE code and CHEMKIN was also excellent, despite the difference in the implemented model (the CHEMKIN model does not operate adiabatically).

Performance comparisons were only possible with DETCHEM^{BATCH} since a copy of CHEMKIN was not at hand. In the comparison described in section 3.4.1, the ENGINE code performed significantly better than the BATCH code. On average, the simulations were completed almost 22 times faster.

4. Application of the Computer Program

4.1. Simulation Settings

Here, an overview of the simulation settings that were used in this thesis is given. All simulations were carried out using the "GRI-Mech 3.0" reaction mechanism [21], developed by the Gas Research Insitute (GRI). The mechanism is widely known and is used to model the combustion of natural gas under various conditions. It considers 53 gas-phase species up to C_3 and includes 325 reactions. The mechanism was optimized for methane and natural gas as fuel in the temperature range of 1000 K to 2500 K (727 °C to 2227 °C), for pressures up to 10 atm and equivalence ratios between 0.1 and 5.0 in premixed systems [22]. Since the optimization was done primarily with natural gas combustion in mind, it is recommended that the mechanism should not be used to simulate fuels with a main component other than methane (e.g. ethane, propane, methanol, ethylene and acetylene) [22].

Table 4.1 shows the fuel and air compositions used in the simulations. The composition of the natural gas is adopted from the publication by Morsy [12]. The composition of the air is based on the numbers given in the textbook "Atmospheric Science" [23], though only considering the three major constituents N_2, O_2 and Ar. Species in the low and sub ppm range such as CO_2 (380 ppm), Ne (18 ppm) and N_2O (0.3 ppm) are neglected. Due to the strongly varying water vapor contents in air (approx. 10 ppm in cold regions of the atmosphere, up to 5 % in hot regions), it is common practice to list the components in relation to dry air [23].

CH_4	C_2H_6	C_3H_8	CO_2	N_2
94.8 %	3.28 %	1.2 %	0.53 %	0.19 %

(a) Natural gas

O_2	N_2	Ar
20.95 %	78.12 %	0.93 %

(b) Simplified dry air (SDA)

Table 4.1.: Composition of the fuel and air used in the simulations.

The geometrical parameters of the simulated engine are shown in Table 4.2. These values are again adopted from the reference article published by Morsy [12]. Since the program developed in this thesis does not directly accept some of the parameters that are given in the article as input values, they must be converted to the correct form. For example, Eq. (2.35) can be rearranged such that the clearance volume can be calculated from the compression ratio and the displacement volume. The crank radius is calculated

with Eq. (2.38) and the ratio of the connecting rod to crank radius is given by Eq. (2.37).

Bore B	85.5 mm
Stroke L	110 mm
Displacement volulme v_d	631.56 cm^3
Compression ratio r_c	17
Connecting rod length l	267 mm
Clearance volume v_c	39.4725 cm^3
Crank radius a	55 mm
Ratio of connecting rod to crank radius R	4.8545

Table 4.2.: Geometrical parameters used in the simulations of the engine. The parameters below the horizontal line denote values that were not present in the reference document but calculated therefrom.

4.2. Autoignition Behavior

In a first step to validate the model implemented in DETCHEM$^{\text{ENGINE}}$, autoignition behavior was analyzed. As can be seen in Fig. 4.1 the reaction system is very sensitive to temperature changes. Both diagrams in the figure show results from simulations that were run with an equivalence ratio of 2.5, 1000 rpm and a pressure of 1.0 bar. In the top diagram, the intake temperature was set to 462 K while the lower diagram shows results with 463 K. A change in one degree of temperature determines whether the mixture ignites or not, a behavior that is also found in experiments [10, 11].

4.3. Pressure Profile: Experiment vs. Simulation

Subsequent to the qualitative considerations, quantitative comparisons were made. As stated in the introduction, not much has been published regarding the use of internal combustion engines as chemical reactors. Thus, it is difficult to find experimental data for partial oxidation conditions that provide enough information to allow simulations to be conducted.

No experimental data was found under fuel-rich conditions. Therefore, the experimental data from a publication by Fiveland et al. was used [5]. In their study, they investigated the sensitivity of HCCI engines to fuel compositions regarding autoignition characteristics under fuel-lean conditions. Although their experiments were not carried out under partial oxidation conditions, they nevertheless provide useful data for a meaningful comparison.

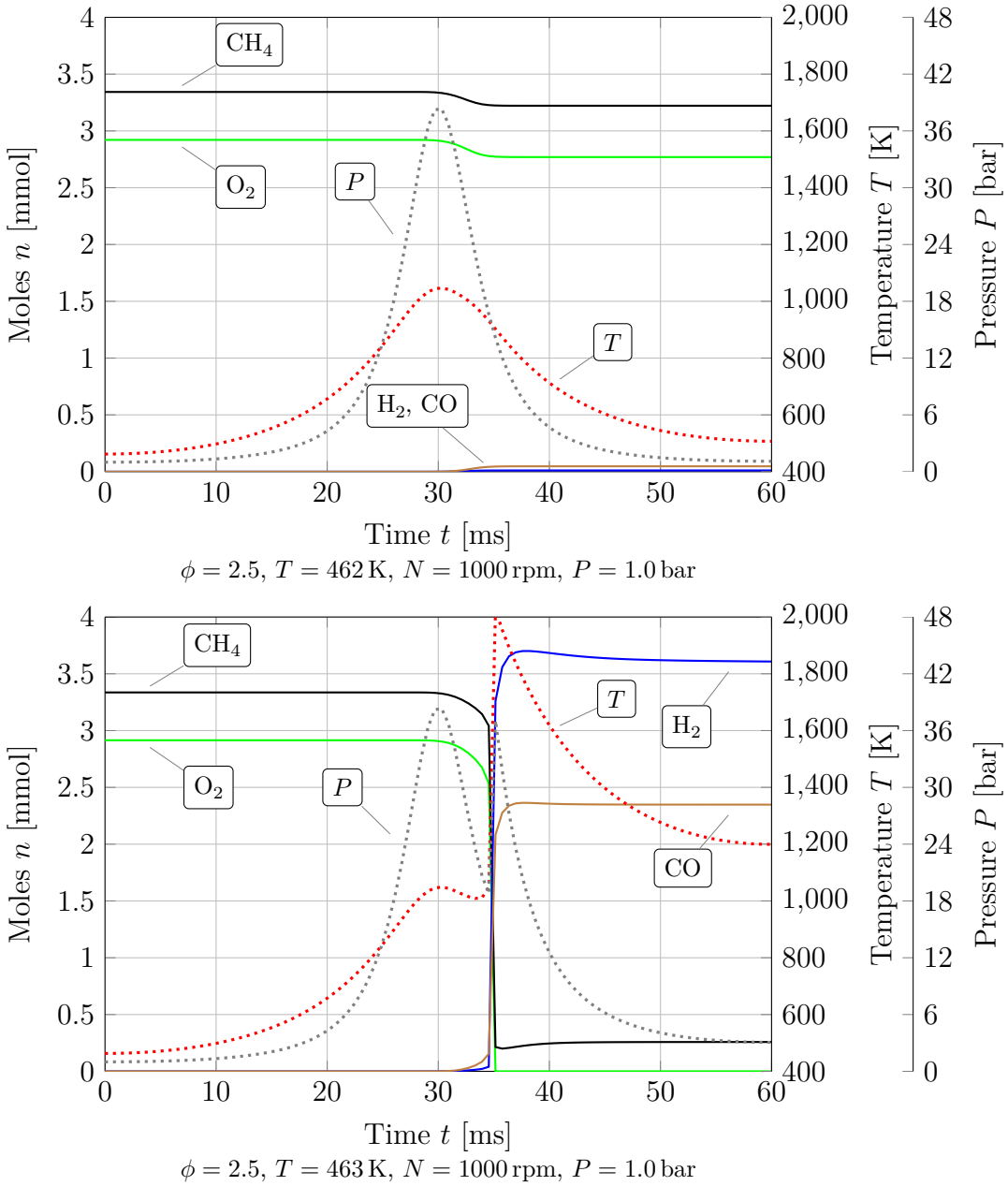

Figure 4.1.: Reaction progress showing moles, temperature and pressure as functions of time for two temperatures near the autoignition limit. Autoignition occurs at an intake temperature of 463 K (bottom), while autoignition fails at an intake temperature of 462 K (top).

Fiveland et al. presented both experimental and modeling results. In their experimental study, they used a custom fitted Volvo diesel truck engine (Volvo TD100), which was modified for single cylinder operation. The cylinder's geometry is shown in Table 4.3. A two component fuel mixture of 99 % CH_4 and 1 % C_3H_8 was used together with an air that was not specified and was thus assumed to be dry air (see Table 4.1). The engine was operated at a speed of 1000 rpm and with an equivalence ratio of 0.3.

Bore B	120.65 mm
Stroke L	140 mm
Compression ratio r_c	19.8
Connecting rod length l	260 mm
Clearance volume v_c	85.136 cm^3
Crank radius a	70 mm
Ratio of connecting rod to crank radius R	3.7143

Table 4.3.: Geometrical parameters used in the simulation of the Volvo TD100 engine used by Fiveland et al. [5]. The parameters below the horizontal line denote values that were not present in the publication but calculated therefrom.

Fig. 4.2 shows the temporal pressure profile of the experiments plotted along with the simulation results from DETCHEM$^{\text{ENGINE}}$. As can be clearly seen in the figure, both the maximum pressure and the time of ignition are not reproduced correctly. The simulation predicts autoignition to occur at approx. 28.7 ms ($\theta = -8$). In the experiment, the mixture ignites shortly after reaching the top dead center, i.e. after 30.0 ms ($\theta = 0$). Furthermore, the pressure progression with time is at all times predicted to be higher than in reality. This is especially apparent after the chemical reaction sets in and the peak pressure is reached. In case of the simulation, the maximum pressure is 95.8 bar. In the experiment, the pressure peaks at only 72.1 bar. This is a difference of 23.7 bar, corresponding to an overshoot of 33 %. However, the model does reproduce the experiment qualitatively, which is reflected by the similar shape of the curves.

4.4. Detailed Analysis of the Reaction Progress

The comparisons between experimental data and simulations described in sections 4.2 and 4.3 have indicated that the computer program DETCHEM$^{\text{ENGINE}}$ produces meaningful results. In a next step, the program was used to gain further insights into the details of a selected reaction.

The detailed reaction progress of the partial oxidation of natural gas is shown in Fig. 4.3. A configuration ($\phi = 3.0$, $N = 1000$ rpm, $T = 530$ K, $P = 1.0$ bar) with a high yield of synthesis gas was chosen for this presentation. The diagram shows the amount of substance as a function of time. For clarity, a second x-axis showing the crank angle

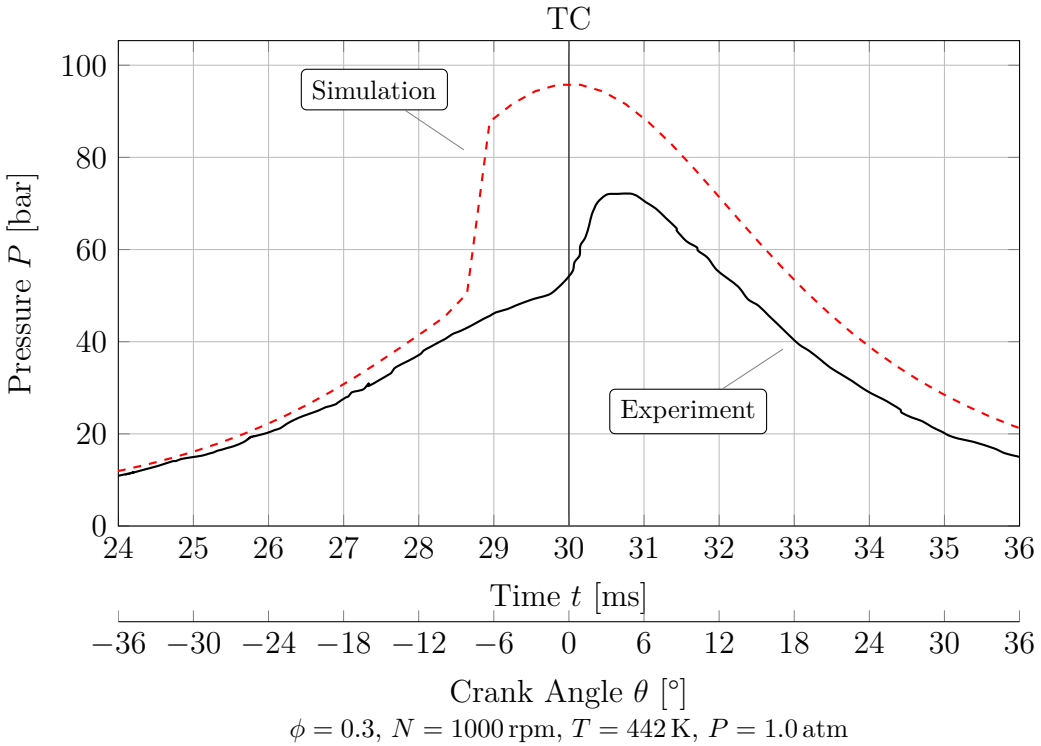

Figure 4.2.: Comparison between model and experiment showing a close-up of the pressure as a function of time and crank angle (adopted from [5], Fig. 3a).

is shown. Furthermore, the temporal temperature profile is plotted. Only a time period of 5 ms (30° crank rotation) during which chemical reaction occurs is shown. At an engine speed of 1000 rpm, the time required to complete one full revolution of the crank is 60 ms.

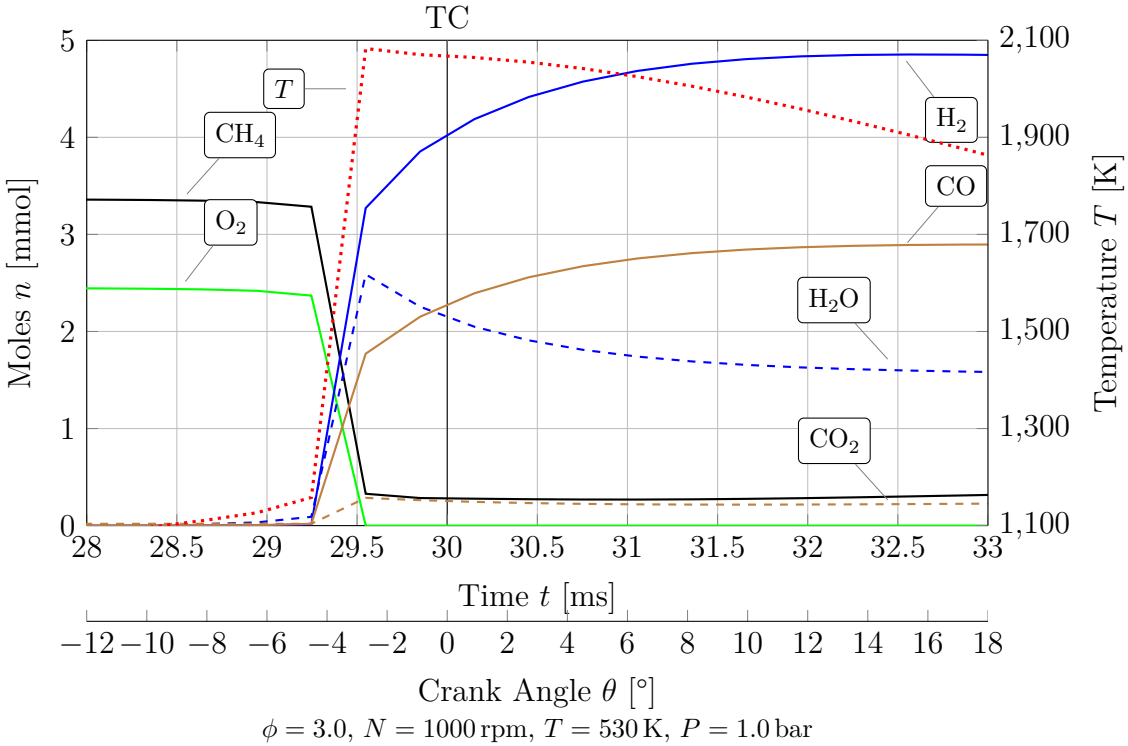

Figure 4.3.: Close-up of reaction progress showing moles and temperature as a function of time and crank angle. The solid lines represent partial oxidation products, the dashed lines represent full combustion products and reactants and the thick red dotted line is the temperature.

It can be seen in Fig. 4.3 that the reaction proceeds via two stages, consistent with previous results [10, 12, 24]. The first "fast" stage begins with the autoignition, which, in this case, occurs at a crank angle of approximately −4.5° ($t = 29.25$). In a time period of approx. 0.3 ms, all of the oxygen is consumed and products of both partial oxidation and full combustion are formed. During this time, there is a dramatic increase of both temperature and pressure. A considerable temperature jump of 924 K from 1158 K to 2082 K takes place. After the first stage ($\theta = -3°$), the amount of H_2O and CO_2 reach their maximum values with 2.59 mmol and 0.29 mmol, respectively (see Table 4.4). In the "slow" stage, the full combustion products (H_2O and CO_2) are then partly converted to the partial oxidation products H_2 and CO. Addionally, methane concentrations rise steadily.

These findings are in agreement with the results of kinetic analyses found in the

	n_{H_2}	n_{CO}	n_{H_2O}	n_{CO_2}	$n_{C_2H_2}$	$n_{C_2H_4}$
$t = 29.55\,\text{ms}$ (stage 1)	3.2715	1.7710	2.5883	0.285 72	0.632 94	0.040 284
$t = 33.17\,\text{ms}$ (stage 2)	4.8456	2.8965	1.5787	0.228 50	0.121 06	0.024 756
$t = 60.00\,\text{ms}$ (exhaust)	4.7387	2.8798	1.5464	0.253 05	0.049 153	0.053 123

$\phi = 3.0$, $N = 1000\,\text{rpm}$, $T = 530\,\text{K}$, $P = 1.0\,\text{bar}$

Table 4.4.: Mole numbers of selected species for three different times of a selected reaction. All values are in mmol.

literature [10, 12, 24]. J. Zhu and coworkers investigated the effects of equivalence ratio, operating temperature and pressure on the production of synthesis gas [24]. For this purpose, a one-dimensional laminar-flow reactor was simulated using CHEMKIN as a simulation tool and the "GRI-Mech 1.2" mechanism. A temperature ramp along the length of the reactor was configured. They found that the reaction proceeds in two distinct *zones*. The term "zone" is probably used because they simulated a *spatially* resolved flow reactor. In the context of this thesis, the term "stage" is more fitting, since a *temporally* resolved reaction system is examined. The reactions thought to occur [24] in the latter zone are steam reforming

$$CH_4 + H_2O \rightleftharpoons CO + 3\,H_2 \qquad \Delta H^\ominus = 205.9\,\text{kJ mol}^{-1}\,, \qquad \{4.1\}$$

water-gas shift reaction

$$CO + H_2O \rightleftharpoons CO_2 + H_2 \qquad \Delta H^\ominus = -41.2\,\text{kJ mol}^{-1}\,, \qquad \{4.2\}$$

methane coupling

$$CH_4 + CH_4 \rightleftharpoons C_2H_2 + 3\,H_2 \qquad \Delta H^\ominus = 376.6\,\text{kJ mol}^{-1}\,, \qquad \{4.3\}$$

and steam reforming of acetylene

$$C_2H_2 + H_2O \rightleftharpoons 2\,CO + 3\,H_2 \qquad \Delta H^\ominus = 35.2\,\text{kJ mol}^{-1}\,. \qquad \{4.4\}$$

In the course of the rest of the cycle (i.e. after the second stage at $t = 33\,\text{ms}$), further conversion of all reaction products occurs. Firstly, the small but steady increase of methane also continues beyond the second stage until the end of the cycle. The mole numbers of H_2, CO and H_2O decrease slightly by 2.2 %, 0.6 % and 2.05 %, respectively while the mole number of CO_2 increases by 10.7 %.

The relative changes of the amounts of C_2-hydrocarbons show the largest change in this phase. C_2H_2 concentrations drop from 0.6 mmol after stage one to 0.05 mmol at the end of the cycle while the amount of C_2H_4 increases from 0.04 mmol to 0.05 mmol. However, the temporal concentration profile of C_2H_4 traverses a minimum near the end

of the second stage, where it reaches a value of 0.025 mmol. Acetylene shows highest concentrations at the end of the first stage and readily reacts during the rest of the cycle.

4.5. Parameter Study: Effect of Equivalence Ratio and Engine Speed Using Different Air Compositions

In this section, the program was used to simulate the behavior of an ICE at high speeds. Furthermore, the effect of replacing nitrogen by argon in the air component was investigated.

Previous research indicates that the yield of synthesis gas can be increased by raising the temperature [10, 12, 24]. According to G. Karim and I. Wierzba, one effect of operating under higher intake temperatures is that the conversion of the fuel is greatly increased [10]. Thermodynamic studies suggest that high temperatures favor the high production of syngas opposed to the full combustion products [24]. This was confirmed by numerical results conducted by M. Morsy [12]. He finds that under very fuel-rich conditions ($\phi = 3.5$) raising the intake temperature leads to higher syngas production. This is shown in Fig. 3.4 on page 31. As can be seen in the figure, the variation of the temperature has a noticable effect on the production of synthesis gas. In the case of $\phi = 3.5$, the production of syngas increases linearly with increasing temperature in the range of the considered temperatures.

Another possibility to raise the temperature is to lower the heat capacity of the reacting mixture. Fig. 4.4 shows the molar heat capacities of nitrogen and argon. Since argon is a mono-atomic gas, its C_P value is very low and independent of temperature. Nitrogen on the other hand is di-atomic. As such, its heat capacity is much higher and exhibits a strong temperature dependency. At 300 K (27 °C) the C_P values of N_2 and Ar are 29.08 kJ mol^{-1} and 20.79 kJ mol^{-1}.

Fig. 4.5 demonstrates the effect of substituting the nitrogen in air completely by argon. The top diagram shows the temporal temperature profile, the bottom diagram shows the pressure profile. The blue lines represent results from simulations run with dry air composition as given in Table 4.1b (simplified dry air, SDA). The red lines represent results from simulations run where the nitrogen in the air was substituted by argon. Hence, the air in the latter case is composed of 20.95 % O_2 and 79.05 % Ar (argon gas mixture, AGM). In order to visualize the effect of the changed heat capacity of the mixture on the temperature, simulations neglecting chemical reactions were also run. These profiles are denoted by the dashed lines. Since both argon and nitrogen are considered to be inert, the substitution of nitrogen by argon does not interfere with the reaction process. Therefore, the difference in all computed quantities can be attributed to the increased temperature only.

The peak temperature difference of 770 K is much higher when chemical reactions are

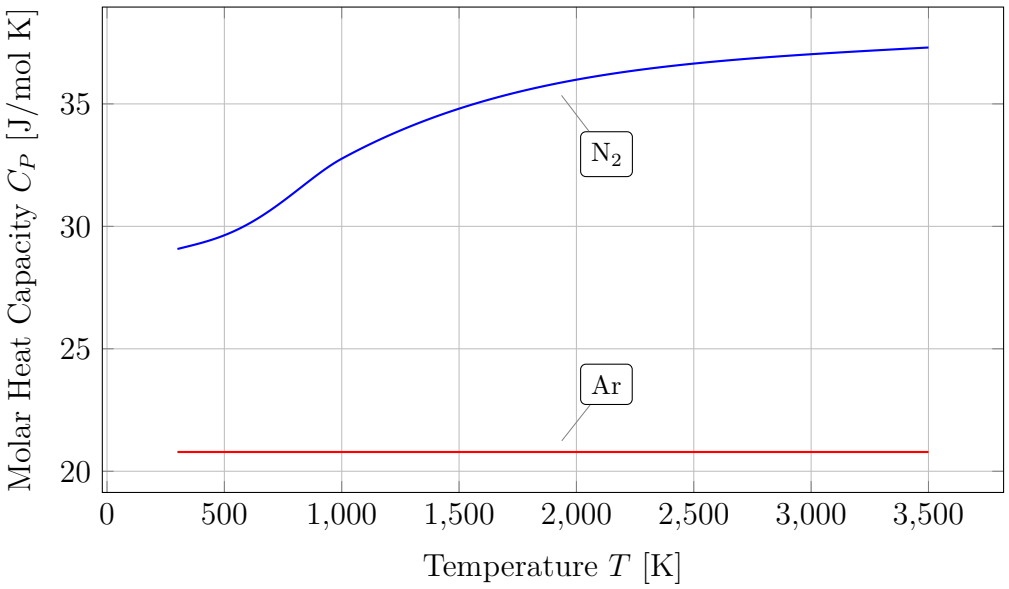

Figure 4.4.: Molar heat capacities as a function of temperature for argon and nitrogen. (Source of the thermodynamic data: Ar [25], N_2 [26]).

accounted for. When reactions are neglected, the temperature difference is only 230 K. This is due to the temperature dependency of the heat capacity of nitrogen. The heat capacity rises with increasing temperature having the effect that more heat can be stored and thus the temperature increase is less.

4.5.1. Effect on Selectivities

The study of selectivities is interesting because it provides insights into which engine configuration will favor the partial oxidation reaction instead of full combustion.

According to M. Morsy's parameter study [12], the configuration with the best syngas production capabilities is at an equivalence ratio of 3.0, 500 rpm, an intake temperature of 530 K and an initial pressure of 1.0 atm. For the following results, intake temperature and initial pressure were set to these values and left unchanged. However, the range of the examined values for ϕ and N were extended considerably. The equivalence ratio was varied from 1.5 to 4.5 in steps of 0.5. For each of these values, simulations with engine speeds from 500 rpm to 3500 rpm in steps of 500 were run. Additionally, an rpm of 250 was investigated. With the same set of settings, the argon air mixture was examined, amounting to a total of 112 simulations that were conducted. Looking into even lower engine speeds did not seem beneficial because it was expected that such speeds are not feasible in conventional engines. Since the production rate of synthesis gas is of particular interest, finding good operating conditions for a given engine speed is insightful.

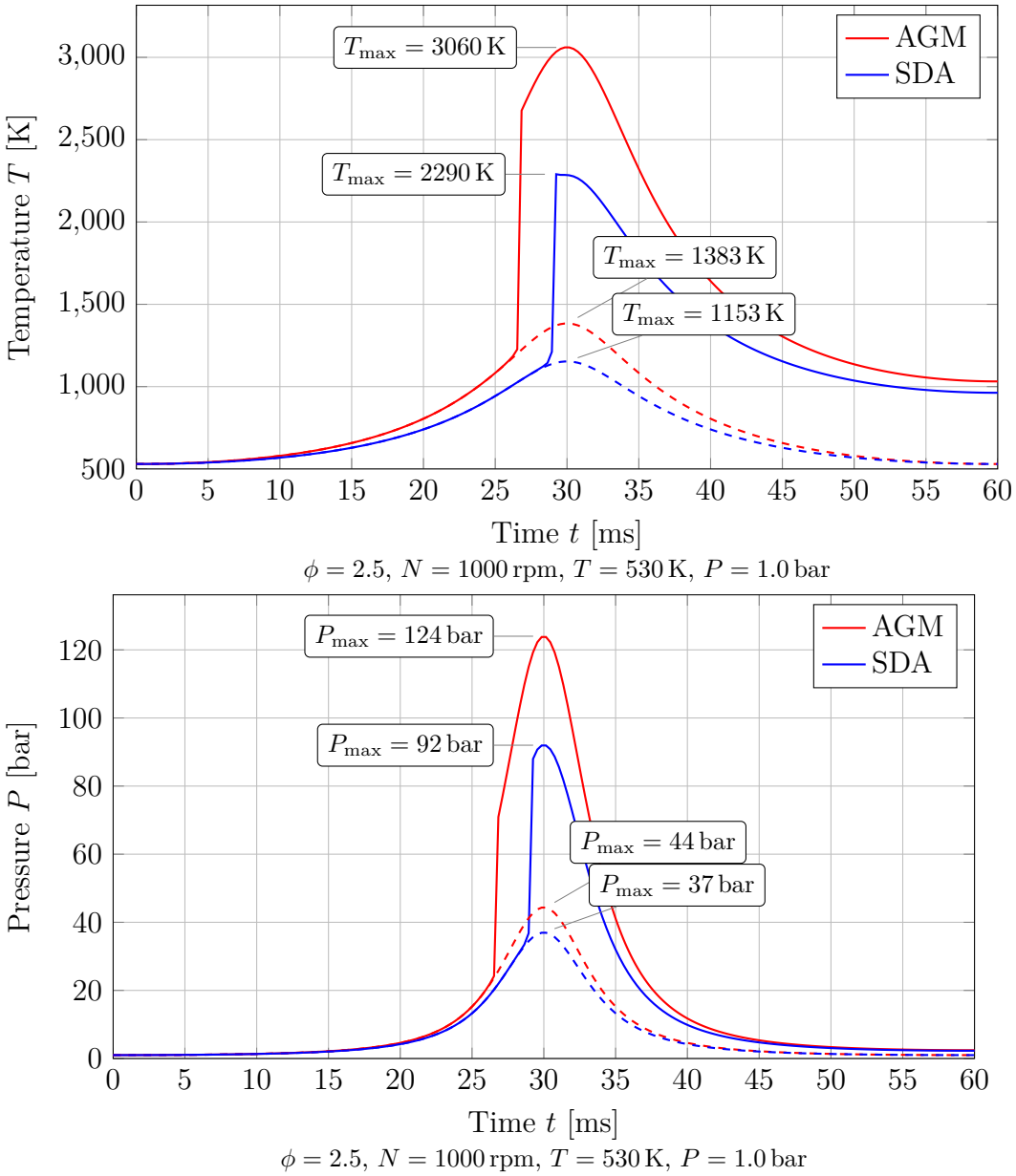

Figure 4.5.: Temperature (top) and pressure (bottom) as functions of time for AGM and SDA, showing the effect of substituting the nitrogen contained in the air component by argon. The dashed lines represent results when neglecting chemical reactions.

The highest selectivities are found to be at 250 rpm and an equivalence ratio of 3.0. When operating the engine under these conditions, the selectivities of H_2 and CO are 85.2 % and 95.5 %, respectively, while converting 98.7 % of the fuel. The selectivities of H_2O and H_2 as well as of CO and CO_2 add up to one, showing that partial oxidation and full combustion are the dominating processes in this system. The yield of other hydrocarbons such as C_2H_2 and C_2H_4 is neglegible, although they do seem to play an important role during the combustion process as shown in section 4.4.

The configuration with highest selectivities when using AGM was found to be at an equivalence ratio of 3.5 and an engine speed of 250 rpm. The selectivity of hydrogen with respect to the fuel is $S_{H_2} = 94.1\,\%$, that of CO is $S_{CO} = 98.6\,\%$ at full conversion. This means that almost all fuel is converted to the desired product syngas, i.e. takes the partial oxidation route.

	X_{fuel}	S_{H_2}	S_{CO}
SDA ($\phi = 3.0$, $N = 250\,\text{rpm}$)	98.7 %	85.2 %	95.5 %
AGM ($\phi = 3.5$, $N = 250\,\text{rpm}$)	100 %	94.1 %	98.6 %

$T = 530\,\text{K}$, $P = 1.0\,\text{bar}$

Table 4.5.: Summary of highest selectivities and corresponding conversions of fuel under SDA and AGM engine operation.

4.5.2. Effect on Production Rate

Fig. 4.6 and 4.7 show the production rate of syngas as a function of engine speed at equivalence ratios of 2.5, 3.0 and 3.5. The first figure shows engine operation with SDA. In the second figure, AGM was used. As expected, the production rate increases more or less linearly with increasing engine speed. In both cases, lowering ϕ leads to a higher linearity. The linearity over a long range signifies that the yield per engine cycle (which is the gradient) is constant and therefore signifies stable operating conditions.

In the case of AGM, using a ϕ-value of 3.5 up to 1500 rpm gives the highest production rate of synthesis gas. At higher engine speeds, a value of $\phi = 3.0$ is more favorable.

However, the SDA simulations show that ignition failures limit the engines operating regions when very fuel rich mixtures are employed. At $\phi = 3.0$, ignition failure sets in at rpms over 2500. In case of an equivalence ratio of 3.5, this is between 2000 rpm and 2500 rpm. These findings are visualized in Fig. 4.8. Ignition failures were not encountered in case of the argon air simulations. Furthermore, preliminary studies (not presented in this thesis) indicated that operation is still possible at 8000 rpm in combination with an equivalence ratio of 3.0.

Of the rpm range explored in this study, the highest production rate could be achieved when running the engine at 3500 rpm and an equivalence ratio of 3.0 with the argon mixture. These results are contrasted with results when running the engine with normal

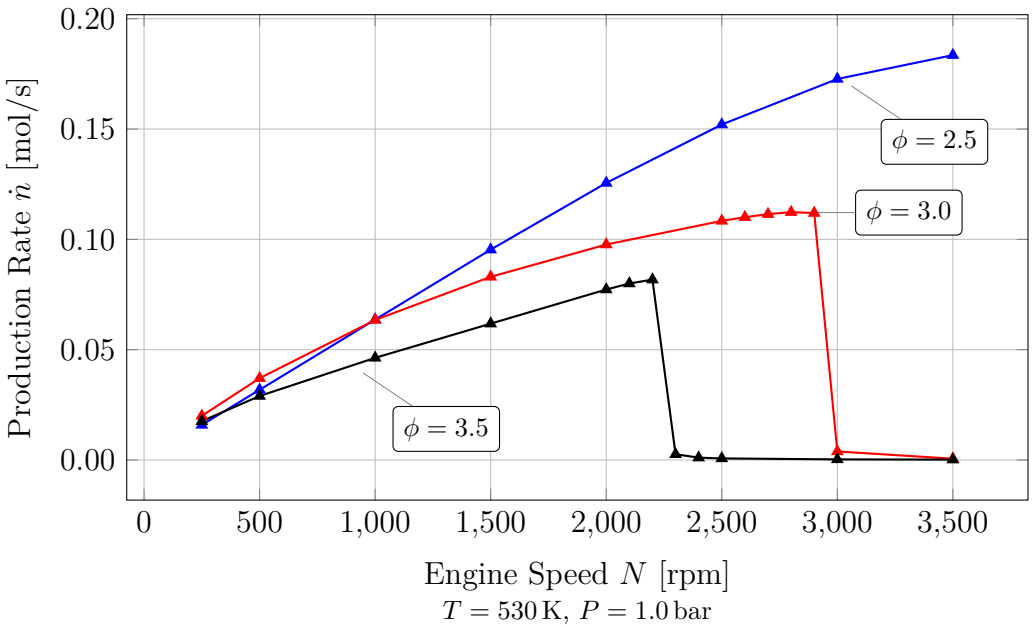

Figure 4.6.: Effect of engine speed on production rate for three different equivalence ratios when using SDA.

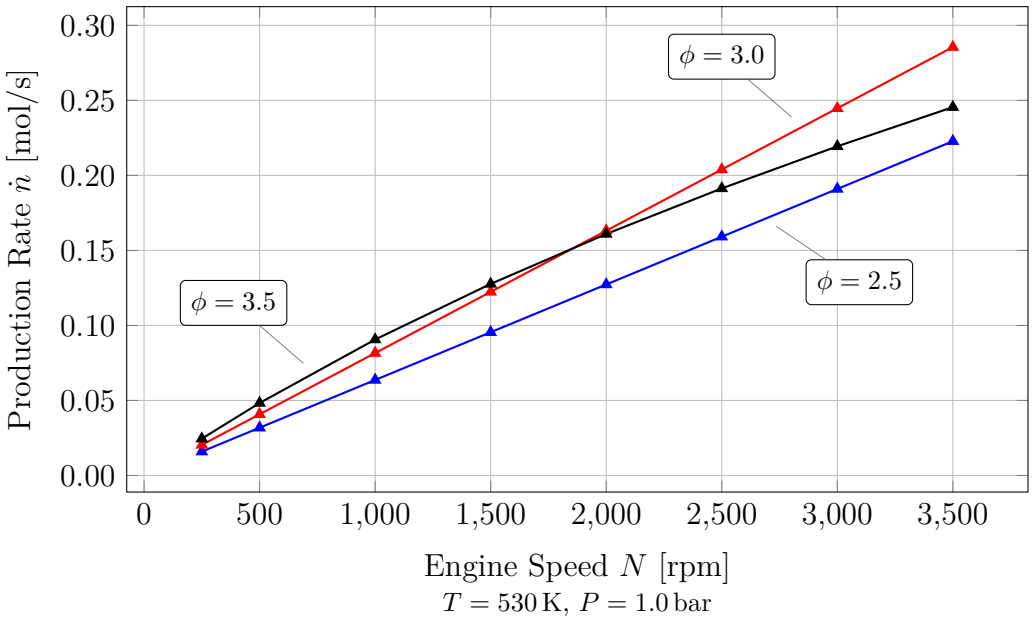

Figure 4.7.: Effect of engine speed on production rate for three different equivalence ratios when using AGM.

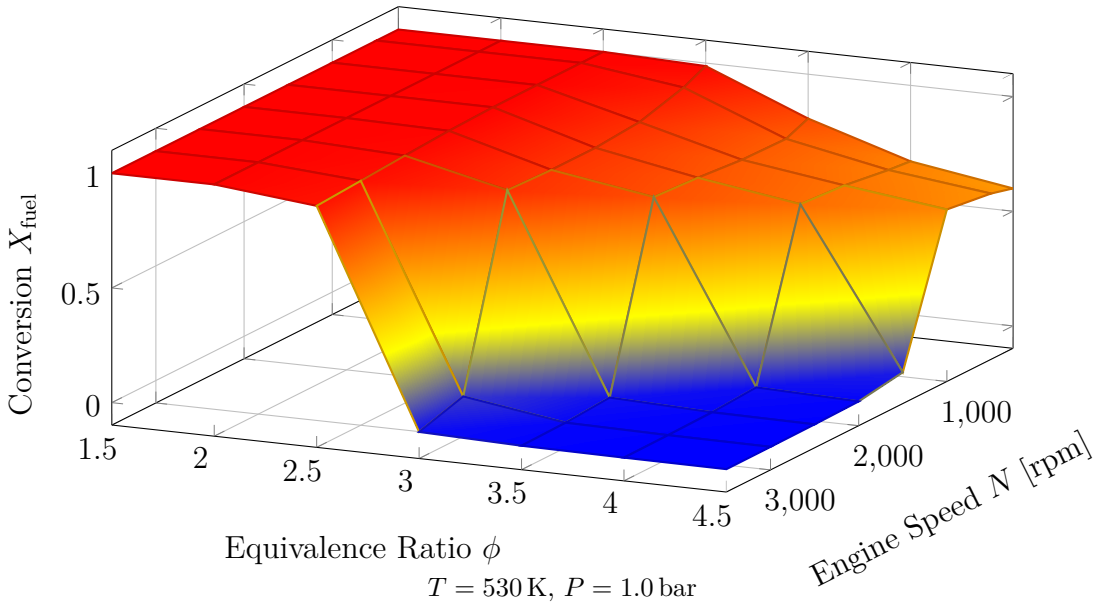

Figure 4.8.: Effect of equivalence ratio and engine speed on the conversion of fuel for SDA, showing the autoignition limit.

air in Table 4.6. The production rate when using AGM is 1.5 times higher than when using SDA. Furthermore, more hydrogen is produced when the engine is operated with AGM.

	$\dot{n}_{\text{syngas}}$	$n_{\text{H}_2}/n_{\text{CO}}$
SDA ($\phi = 2.5,\ N = 3500\,\text{rpm}$)	$0.184\,\text{mol s}^{-1}$	1.53
AGM ($\phi = 3.0,\ N = 3500\,\text{rpm}$)	$0.285\,\text{mol s}^{-1}$	1.72

$T = 530\,\text{K},\ P = 1.0\,\text{bar}$

Table 4.6.: Summary of highest production rates of syngas and corresponding H_2 to CO ratio under SDA and AGM engine operation.

5. Discussion

In this thesis, a new computer program was developed allowing for the simulation of chemical reactions in ICEs. It was used to carry out a parameter study comparing the effect of SDA and AGM on the synthesis gas production under partial oxidation conditions. In the following, the results from this work are discussed.

5.1. Verification of the Computer Program

To eliminate programing errors, DETCHEM$^{\text{ENGINE}}$ was compared with two well established simulation tools. In a first comparison, results of the program DETCHEM$^{\text{BATCH}}$ were considered (see 3.1). Nearly identical results were output by both programs. However, small deviations of mole numbers in the exhaust in the order of 10^{-7} to 10^{-17} exist. A reason for this may be that the volume profile can only be specified in the form of discrete points in the BATCH program (see the input file on page 64 for details), while the ENGINE program uses an algebraic equation (2.36) to compute the volume for a given time. In addition, slightly different settings of the solver used to solve the system of differential algebraic equations can be the cause of the numerical discrepancies. The parameters thought to have the highest impact on precision and performance were set to equivalent values in both programs, others were either left to default values or could not be modified without changing the source code of the BATCH program. The parameters set to equivalent values were absolute tolerance (set to 10^{-20}), relative tolerance (10^{-9}), intial step size guess (10^{-10}) and maximum step size (LIMEX default).

In a second comparison, DETCHEM$^{\text{ENGINE}}$ was compared to CHEMKIN. Interestingly, near exact concordance between the results of both programs was found, despite the slight difference of the implemented models. The CHEMKIN model accounts for the heat exchange between the gas and cylinder walls by employing the Woschni heat transfer correlation while the ENGINE model assumes adiabatic operation. This indicates that the consideration of the heat transfer does not play an important role in this context. This could be studied in more detail in the future by varying the temperature of the engine components, which were kept at a constant value of 450 K in all of the CHEMKIN simulations.

The slight differences that were found between the result sets of the two programs can be attributed to the heat loss that is considered in CHEMKIN only. Furthermore, assumptions were made regarding air composition (see Table 4.1) and intitial pressure (assumed: 1.0 bar) because there was no indication of these values in the publication.

It is unlikely though, that these assumptions would compensate a strong deviation originating from the engine cooling in such a way, that the results are "by coincidence" in such excellent concordance.

Performance comparisons in terms of speed were only possible with DETCHEM$^{\text{BATCH}}$ since a copy of CHEMKIN was not at hand. On average, the ENGINE code completed the simulation almost 22 times faster than the BATCH code. It should be noted however, that further investigations must be made in order to arrive at a well-founded conclusion. For one, performance should also be compared at various conditions (equivalence ratios, intake temperatures, engine geometries, etc.). But more importantly, the solver settings that are hard-coded in the BATCH program should be examined and adjusted, if applicable.

5.2. Model Validation

In a first step to validate the model implemented in DETCHEM$^{\text{ENGINE}}$, autoignition behavior was analyzed. The numerical results showed that the behavior of the autoignition is similar to that found in experiments [10, 11]. An important result from these experiments was the identification of stable engine operating regions. The operating map in the work by Y. Yang et al. was derived by varying intake temperature and equivalence ratio [11]. G. Karim and I. Wierzba identified stable regions with respect to oxygen contents in air and equivalence ratio [10]. The results presented in both reports indicate sharp boundaries between stable and instable operating regions. In other words, there is no smooth transition between conditions under which selfignition occurs and those under absence of selfignition. The simulation results also reproduce a sharp boundary between misfire and autoignition regions. However, the results cannot be compared directly since the engine used in the experiment was not driven externally as was done in the simulation. Under normal engine operation, fuel flow determines engine speed.

Numerical results were in qualitative agreement with experimental data found in the literature. The overall shape of the time-dependent pressure profile was reproduced well. However, the simulation predicts significantly higher pressures than those found in the experiment. The deviation of the pressure before ignition occurs indicates that the ideal gas treatment is a significant cause of error. The pressure offset may be the cause for the early ignition, so that by remedying the pressure overshoot the self ignition problem is also possibly solved. This may also be the reason for the ignition time being predicted as too early since the pressure reaches a critical point earlier as in the ideal gas treatment. Furthermore, the model neglects heat losses. This obviously affects the peak temperature in the cylinder and is certainly another reason for the pressure overshoot. On the one hand, the simulated pressure is higher due to the higher in-cylinder temperature itself. On the other hand, the higher temperature leads to a faster heat release from chemical reactions. Additionally, higher conversions lead to a higher number of species, also effectively increasing pressure.

Finally, the reaction mechanism itself is a possible source of discrepancy between

numerical and experimental results. This is especially true in the conditions encountered in the simulation because the mechanism is not validated at these elevated pressures [22].

The mechanism used is not confirmed to be valid under all the conditions that are reached during the course of an engine cycle. Especially the specified pressure range mentioned in Curran's article [22] of 1 atm to 10 atm was exceeded drastically. The peak pressures encountered in the simulation was nearly 100 bar. This may be a significant source of error, but it cannot be said whether the results presented are predicted to be too high or too low.

5.3. Detailed Analysis of the Reaction Progress

It was shown in Fig. 4.3 (page 38) that the reaction progress proceeds via two stages. A slight temperature decline before reaching TC, i.e. still during the compression in which the temperature should increase, exists. This strongly indicates that endothermal reactions are taking place. Zhu et al. [24] were unable to see such an effect in their analyses, since the model used in their simulation did not include an energy equation.

In the second stage, products of full combustion (H_2O and CO) are consumed and H_2 and CO are formed. These findings support Zhu et al.'s assumption that water-gas shift and steam reforming of C_2H_2 are taking place [24]. In this phase, the temperature is decreasing. Therefore, exothermal reactions are favored while endothermal reactions are not. Steam reforming and methane coupling to C_2H_2 is therefore likely to proceed in the reversed direction as stated above.

Acetylene shows highest concentrations at the end of the first stage and readily reacts during the rest of the cycle. Therefore, acetylene yield is probably highest at very high engine speeds, because the time spent in the slower reforming stages is reduced. The levels of ethylene are highest in the exhaust, or with nearly 80 % of this value at the end of the first stage, but are lowest in between. Hence, highest ethylene yields can be expected at either very high or very low engine speeds. However, the relative concentrations of both described C_2 hydrocarbons is low throughout the whole reaction. Therefore, the production of these species in an ICE can currently not be considered as relevant.

5.4. Parameter Study

In the parameter study, the behavior of an ICE at high speeds was studied. Additionally, the effect of using AGM instead of SDA was investigated. The results indicate that when operating at low engine speeds, it is favorable to use higher fuel-air ratios in order to increase the production rate of syngas than when running the engine at higher rpms. This effect is less pronounced when the engine is operated with SDA. The cause of this behavior is that the selectivity of H_2 and CO is higher at fuel-richer mixtures. However,

the decrease of conversion with increasing engine speed is more pronounced at higher equivalence ratios. These opposing trends eventually compensate each other leading to the "switch" that can be seen in the diagrams.

The results presented in section 4.5.2 indicate promising engine operating conditions for high synthesis gas production rates in an internal combustion engine. However, the parameter study was carried out neglecting technical constraints that would be relevant under practical conditions. These points are discussed in the following and will need to be addressed in future simulations.

Ignition timing. A key issue in engine operation is ignition timing. A likely problem when running the engine with high argon levels is that ignition timing will be more difficult to control. Due to the faster rising temperature, ignition occurs much earlier than when operating the engine with SDA.

The problem of ignition timing has been addressed under conventional conditions [5, 27], but thus far not under rich-fuel conditions when operating with AGM. However, such studies will need to be carried out under these conditions to further evaluate syngas production with AGM from a technical point of view.

Drastic conditions. Numerical results indicated that the engine will be exposed to more drastic peak temperatures and pressures when operated with AGM. These conditions call for a robust engine design. Conventional engines can possibly not be simply custom fitted for such use, making the development of a new engine design necessary specifically for this purpose. This may require a large initial investment that cannot be outweighed by the advantages of AGM operation. However, the large pressure overshoot that was found when comparing the model to the experimental data suggests that the conditions found in the AGM results may not be as drastic in reality as predicted in the simulation. Another source of uncertainty is that the conditions encountered lie beyond the range under which the used mechanism was validated [21, 22]. This may be a significant source of error, but it cannot be said whether the results presented were predicted to be too high or too low.

Soot particle formation. Furthermore, soot particle formation has to be considered. In this respect, contradicting reports in the literature exist. Soot formation was reported by L. von Szeszich, but only under certain conditions [8]. Also, high levels of soot are to be expected under fuel-rich conditions according to Lemke et al. [28]. On the other hand, M. McMillian and S. Lawson did not encounter elevated particulate emissions [9].

In any case, the use of an ICE offers interesting possibilities to possibly circumvent the production of soot which are worth investigating. Since the presence of steam is known to inhibit soot formation [29], the addition of small amounts of steam poses a possibility to reduce the risk of soot formation. The steam could either be premixed with the initial charge or be injected seperately.

Further investigation with respect to soot particle production is limited by the mechanism. For example, the mechanism [21] used throughout this work does not account for particle production.

Water contents. The study of water content of the reacting mixture is in itself an interesting topic. In light of the varying water content in the air [23], further investigation of the effect of steam regarding engine operation characteristics and synthesis gas production is warranted. In particular, the stability of engine operation at high rpms where high production rates of syngas are expected needs further attention.

It can be assumed that the addition of steam will also have a positive effect on the syngas yield. Looking at the water-gas shift reaction ({4.2}, page 39), raising the water concentration will shift the equilibrium towards the product side. This is especially the case at higher temperatures, as is the case when using high amounts of argon. However, adding steam would again increase the heat capacity of the reacting mixture, leading to lower temperatures. The resulting lower temperatures will again have a negative impact on syngas production. It can therefore be expected that, due to these opposing trends, an optimal steam content of the reacting mixture will exist with respect to highest syngas production.

Low fuel conversions. Lower fuel conversions were especially encountered when operating with SDA. A possible remedy for these low conversions is exhaust gas recirculation. However, this will have no effect on the production rate of the engine. In this respect, the use of AGM shows superior characteristics.

6. Conclusion and Outlook

In this thesis, a computer program named DETCHEM$^{\text{ENGINE}}$ was developed to describe the chemical conversion inside a cylinder of an internal combustion engine. The incorporated model corresponds to an idealized batch reactor with a variable volume profile and is based on detailed gas-phase reaction mechanisms. With this program, time-dependent concentration profiles were calculated from which product compositions, yields and selectivities were derived. By comparing the computer program developed in this thesis with widely used commercially available software, it could be shown that it is capable of producing accurate results. In summary, the following results can be stated:

Program verification. In order to eliminate programing errors, the results from the computer program were verified by comparing them to results obtained by two other existing programs: DETCHEM$^{\text{BATCH}}$ and CHEMKIN. All results obtained with DETCHEM$^{\text{ENGINE}}$ are in excellent concordance to those generated with either of the other programs.

First, a comparison was made against DETCHEM$^{\text{BATCH}}$, a program which is part of the DETCHEM software package [14]. Both programs output nearly identical results. However, DETCHEM$^{\text{ENGINE}}$ completed the simulation almost 22 times faster than DETCHEM$^{\text{BATCH}}$.

In a second comparison, results from the commercially available CHEMKIN software package were used. The agreement between the ENGINE program and CHEMKIN was also excellent, despite the difference in the implemented models (the CHEMKIN model does not operate adiabatically). This indicates that the Woschni heat transfer correlation is not of significant importance in this context.

Model validation. The underlying model corresponds to an idealized batch reactor with a variable volume profile. It was validated by comparing results to experimental data described in the literature. Numerical results were in qualitative agreement with experimental results found in the literature. Autoignition behavior and the overall shape of the temporal pressure profile is reproduced well. However, the simulation predicts significantly higher pressures than those found in the experiment. The most likely cause of this overshoot is assumed to be the ideal gas treatment in the model.

Simulation results. The detailed reaction progress of a selected simulation was analyzed. The analysis showed that the concentrations of acetylene and ethylene were low throughout the reaction progress compared to those of the partial oxidation or full combustion

products. However, the temporal concentration profiles suggested that changing engine speed can have a positive effect on the yield of these species.

Furthermore, promising operating conditions for the production of synthesis gas in an internal combustion engine were identified by a parameter study. The study focused on production rates and selectivities of H_2 and CO with respect to the fuel.

In general, the use of argon gas mixture (AGM: 20.95 % O_2, 79.05 % Ar) instead of simplified dry air (SDA: 20.95 % O_2, 0.93 % Ar 78.12 % N_2) led to much higher fuel conversions and selectivities of H_2 and CO with respect to the fuel. Furthermore, the higher the fuel enrichment of the feed, the lower the fuel conversion. Main results of the parameter study are:

- The use of AGM instead of SDA resulted in an a 1.5 fold increase of the syngas production rate in combination with a H_2 to CO ratio of 1.72 rather than 1.53.
- When AGM was used, the operating conditions under which the highest selectivities achieved were $\phi = 3.5$, $N = 250\,\text{rpm}$, $T = 530\,\text{K}$, $P = 1.0\,\text{bar}$. Selectivities: $S_{H_2} = 94.1\,\%$, $S_{CO} = 98.6\,\%$ at full conversion.
- When SDA was used, the operating conditions under which the highest selectivities achieved were $\phi = 3.0$, $N = 250\,\text{rpm}$, $T = 530\,\text{K}$, $P = 1.0\,\text{bar}$. Selectivities: $S_{H_2} = 85.2\,\%$, $S_{CO} = 95.5\,\%$ at 98.7 % conversion.

These results show that the use of argon-enriched air poses a new possibility to produce large amounts of synthesis gas in an ICE. In addition, this mode of operation is far less prone to autoignition failures than the operation under SDA.

Technical constraints. The parameter study was caried out neglecting technical constraints that would be relevant under practical conditions. Future simulations will need to address these points, of which ignition timing and soot particle production are essential. They were not investigated further in this work because the current model is a simplified model, which does not provide well-founded insights in this direction. Therefore, a refinement of the model is necessary to address these issues. However, this was beyond the scope of this work.

In future work, non-ideal gas effects need to be considered. Furthermore, while heat loss does not have a large impact on product compositions, it may however play an important role within the scope of ignition timing. Therefore, it will be also be important to study the effect of engine cooling on ignition timing under partial oxidation conditions.

In addition, in the current model implementation the engine is forced to run at a given speed. This corresponds to an externally driven engine which does not reflect realistic engine operating conditions. Hence, in order to evaluate the system from a more profound technical view, the model needs to be extended such that the engine speed is a result of the chemical reaction in the cylinder. This implies a multi-cycle simulation with many iterations until a steady state is reached. Futhermore, additional

engine parameters will be needed, such as mass of moving parts and internal friction. Such an implementation of the model will also open new possibilities for quantitative model validations against experiments. In the publications by Fiveland and Assanis [30, 31] such a multi-cycle simulation tool is presented. These articles can provide insight to such an implementation, also including a non-ideal gas model.

Mathematical optimization. With the presented parameter study, promising operating conditions for high synthesis gas production were identified. However, the study has only scratched the surface of possible parameter combinations. In this thesis, it became clear that even a numerically conducted parameter study by means of "trial and error" methods is not practical. For example, for the results presented in the parameter study, 120 simulations were run and evaluated. A next step is therefore to find the optimal engine configuration for desired operating characterstics by means of mathematical optimization.

One conceivable objective function of such an optimization problem would be the maximization of the yield of a desired product together with the overall efficiency of the process. The evaluation of the efficiency would need to include energy in the form of heat, power and chemicals. For meaningful results, constraints will need to be introduced that consider technical specifications including those outlined above. However, engine speed and geometrical parameters are also subject to restrictions.

Primarily the initial conditions can be used as control parameters of the optimization. This is because not much influence can be exerted on the system during the compression and expansion stroke.

The evaluation of the objective function involves solving a coupled differential algebraic equation system, which is computationally expensive. Therefore, the choice of the most suitable optimization algorithm is essential in order to arrive at a solution in a reasonable amount of time. This will be especially important with a more complex model, which implies even longer computational times.

The computer program presented in this thesis will provide the foundation for further work in this direction. The model will be extended to reduce the shortcomings that were describe in this section. The program will be further developed in order to facilitate the mathematical optimization of operation parameters to find the optimal conditions, at which the desired product yield and energy efficiency is maximized.

A. Manual for DETCHEM$^{\text{ENGINE}}$

DETCHEM$^{\text{ENGINE}}$ is a computer program written in Fortran for the simulation of homogeneous gas-phase reactions in an internal combustion engine. The compression and expansion strokes are mimicked by means of a time-dependent volume profile, which is derived from geometrical parameters of the engine. It is possible to specify seperate fuel and air compositions.

A.1. Governing Equations

A summary of the governing equations of the underlying model are given below.

$$Pv = nR_0T \qquad \text{(Ideal gas law)}$$

$$\frac{\mathrm{d}n_i}{\mathrm{d}t} = v \cdot \dot{\omega}_i \qquad \text{(Gas-phase species)}$$

$$\frac{\mathrm{d}T}{\mathrm{d}t} = \frac{\sum_i [\dot{n}_i \Delta H_i(T) - \dot{n}_i R_0 T] - P\dot{v}}{\bar{c}_v} \qquad \text{(Energy balance)}$$

$$v = v_\mathrm{c} \cdot \left(1 + \frac{1}{2}(r_\mathrm{c} - 1)\left[R + 1 - \sqrt{R^2 - \sin^2\theta} - \cos\theta\right]\right) \qquad \text{(Volume profile)}$$

The variables above denote

P: pressure
v: volume
n: species moles
R_0: universal gas constant
T: temperature
$\dot{\omega}$: gas-phase reaction rate
v_c: clearance volume
r_c: compression ratio
R: connecting rod length to crank radius ratio
θ: crank angle
N: engine speed

The index i signifies the species. The implicit solver LIMEX [19] is used to solve the system of differential algebraic equations.

A.2. Compiling from Source

When unpacked, the main directory contains the following files and directories:

```
path/to/detchem/ <– the directory the source was extracted to
  config/
    system.mk.dist
    ...
  lib/
    detchem/
    limex/
    ...
  run/
    engine/
    ...
  src/
    engine/
      config.f95
      main.f95
      makefile
      output.f95
      physical_constants.f95
      solver.f95
  tools/
    configure.py
    template.dist/
  ...
```

After obtaining the source code, system specific settings must be configured before the program can be compiled. For convenience, the package contains a template which can be copied and adapted:

```
cp config/system.mk.dist config/system.mk
```

Then the `system.mk` file in the `config/` directory must be edited. The `GFORTRAN` variable should be set to the absolute path of the `gfortran` compiler. Next, the command

```
make engine
```

results in a `release` build, or

```
make engine CFG=DEBUG
```

results in a `debug` build. In the latter case, the compiler flags to allow for interactive debugging are set. After the compilation has completed, the `engine` executable can be found in a subdirectory named `release/` or `debug/` within the `bin` directory. Since binaries and object files for both compiler configurations are put into separate locations, issuing the `make clean` command when switching between `debug` and `release` builds is not necessary. Running `make` directly from the `engine` directory will result in an error.

```
{include species.inp}
{include mech.inp}

<ENGINE>
  pressure = 1.0d5
  temperature = 300
  clearance_volume = 100d-6
  compression_ratio = 15
  connecting_rod = 250 [mm]
  crank_radius = 50 [mm]
  rpm = 1000
  equivalence_ratio = 1.0

  <FUEL_COMPOSITION>
    CH4   *
    C2H6  0.01
  </FUEL_COMPOSITION>

  <AIR_COMPOSITION>
    O2    0.2095
    Ar    0.0093
    N2    *
  </AIR_COMPOSITION>
</ENGINE>
```

Listing A.1: Example of input file `engine.inp` for engine

A.3. User Input

Before running DETCHEM$^{\text{ENGINE}}$, the user must prepare an input file `engine.inp`. An example is given in Listing A.1 Typically, the files in working directory include:

```
engine.inp
species.inp
mech.inp
mechanism
thermdata
moldata
```

See chapters 2 and 3 of the DETCHEM manual for an in-depth explanation of supported rate expressions and the mechanism file format. The following options are required and must be specified with the `engine` tag:

`pressure = d` initial pressure P [Pa]
`temperature = d` intake temperature T [K]
`clearance_volume = d` clearance volume of the cylinder v_c [m^3]
`compression_ratio = d` compression ratio r_c
`connecting_rod = d` length of the connecting rod l [m]
`crank_radius = d` crank radius a [m]

equivalence_ratio = d equivalence ratio ϕ

All parameters above are of type `double` which is denoted by the `d`. The equivalence ratio must be set to be greater than 0. The composition of the fuel and air are entered within the `FUEL_COMPOSITION` and `AIR_COMPOSITION` tags in the form as shown in the example. The current implementation accounts for fuels consisting of carbon, hydrogen, oxygen and sulfur. The mole fraction of oxygen (`O2`) in the air component must be greater than zero. The `engine.inp` file starts with the species and mechanism definition section, that can appear directly in the input file or can be included from external files via the `include` command as shown in the example. In addition, the files `thermdata` and `moldata` must be located in the working directory.

Solver settings are currently hard coded and cannot be set via the input file. In order to change these, the user must edit the source code and recompile. The relevant file is `src/engine/solver.f95`.

A.4. Program Output

The program writes the output to a file named `result.plt` in the current working directory. This file contains values of pressure, volume, temperature and mole numbers of all involved species for a given time. The format of the file is fixed-width columns, which is a common format and can therefore be imported into most programs for further evaulation and analysis. Tools are included that facilitate the evaluation (see below). Additionally, the program outputs the integration progress to the console.

A.5. Running the Program

It is recommended to create separate directories for each simulation run. The directory must contain all the input files mentioned above. After changing to the directory containing the input files, the program is executed from the command line:

```
cd path/to/simulation_directory
path/to/detchem/bin/release/engine
```

A.6. Supplemental Tools

Several tools to facilitate easy evaluation of the simulation results are included.

A.6.1. Configuration from Templates

Furthermore, a tool is available to setup new problems from a template. This allows for rapid execution of simulations with similar settings, ideal for parameter studies. First, the template must be created. From within the `DETCHEM` directory:

```
cp -R tools/template.dist tools/template
```

The contents of the created `template` directory can then be edited according to the users needs. It is important that the format of the `engine.inp` file stays intact. Note the curly braces. Additionally, default values are set in the `configure.py` script. The `dict` that is defined at the top of this file shows the default values. If the value is not set from the command line, the default value will be used. Note that the values of the `dict` must be of type `string` as shown in the example.

```
params = {
    'pressure': '1.0d5',
    'temperature': '530',
    'clearance_volume': '39.4725d-6',
    'compression_ratio': '17',
    'connecting_rod': '267',
    'crank_radius': '55',
    'rpm': '1000',
    'phi': '2.5'
}
```

These values can then be conveniently set from the command line:

```
cd simulations/
detchem/tools/configure.py temperature=500
```

The script creates a new directory according to a naming convention shown in the console output below. The settings given in the command line as arguments are merged with files from the `template` directory and are copied to the new directory. Provided that the template files were not malformed, DETCHEM$^{\text{ENGINE}}$ can be run from this directory. The command above outputs:

```
cd simulations/
detchem/tools/configure.py temperature=500
```

This prints the following to the command line, showing which files were created in the new directory. Additionally, the name of the dir that got created can be seen.

```
template -> phi2.5-N1000rpm-T500K-P1.0bar
template/engine.inp -> phi2.5-N1000rpm-T500K-P1.0bar/engine.inp
template/figures -> phi2.5-N1000rpm-T500K-P1.0bar/figures
template/gm_GRI30 -> phi2.5-N1000rpm-T500K-P1.0bar/gm_GRI30
template/gnuplot.conf -> phi2.5-N1000rpm-T500K-P1.0bar/gnuplot.conf
template/mech.inp -> phi2.5-N1000rpm-T500K-P1.0bar/mech.inp
template/moldata -> phi2.5-N1000rpm-T500K-P1.0bar/moldata
template/result.plt -> phi2.5-N1000rpm-T500K-P1.0bar/result.plt
template/species.inp -> phi2.5-N1000rpm-T500K-P1.0bar/species.inp
template/thermdata -> phi2.5-N1000rpm-T500K-P1.0bar/thermdata
```

In an analogous fashion, the command

```
detchem/tools/configure.py temperature=450 phi=0.5
```

creates the configuration files for an intake temperature of 450 K and an equivalence ratio of 0.5 in the directory`phi0.5-N1000rpm-T450K-P1.0bar`.

A.6.2. Evaluation Tools

The tools `mole_fractions_exhaust.py`, `moles_exhaust.py` and `selectivity.py` can be run from the command line. These scripts expect the presence of a `result.plt` file in the working directory.

B. Input Files

The input files shown here were used in the comparison between DETCHEM$^{\text{ENGINE}}$ and DETCHEM$^{\text{BATCH}}$. When run with these settings, both programs output nearly identical results.

B.1. DETCHEM$^{\text{ENGINE}}$

```
{include species.inp}
{include mech.inp}

<ENGINE>
  pressure = 1.0d5
  temperature = 500
  clearance_volume = 39.4725d-6 # 1 cm3 = 1d-6 m3
  compression_ratio = 17
  connecting_rod = 267 [mm]
  crank_radius = 55 [mm]
  rpm = 1000
  equivalence_ratio = 2.5

  <FUEL_COMPOSITION>
    # Morsy 2014 natural gas composition
    CH4   0.948
    C2H6  0.0328
    C3H8  0.012
    CO2   0.0053
    N2    0.0019
  </FUEL_COMPOSITION>

  <AIR_COMPOSITION>
    # Dry air
    O2    0.2095
    AR    0.0093
    N2    *
  </AIR_COMPOSITION>
</ENGINE>
```

B.2. DETCHEM^{BATCH}

```
{include species.inp}
{include mech.inp}

<BATCH>
  solver_id = 0
  p= 1.0d5 [Pa]

  <MOLEFRAC>
     CH4    0.191368445416
     C2H6   0.0066211867125
     C3H8   0.00242238538987
     CO2    0.00106988688084
     O2     0.167209188671
     AR     0.00742265134811
     N2     0.623886255582
  </MOLEFRAC>

  time=0.06

  h=1.e-10
  atol=1.e-20
  rtol=1.e-9

  <CONST_QUANTITY>
    T/K = 500
    const_quantity = Q
  </CONST_QUANTITY>

  <OUTPUT>
    mole = y
    concentration = n
    mole_fraction = n
    mass_fraction = n
    fileNr=1
    dt_out=0.0003 # about 200 data points in output file
    monitor = 1
  </OUTPUT>

# N = 1000rpm, compression_ratio = 17
# connecting_rod = 267 [mm], crank_radius = 55 [mm]
  <V_PROFILE>
0.00000000E+000   6.71032500E-004
3.01507538E-004   6.70907525E-004
6.03015075E-004   6.70532631E-004
9.04522613E-004   6.69907915E-004
1.20603015E-003   6.69033536E-004
1.50753769E-003   6.67909721E-004
```

```
48 1.80904523E-003   6.66536764E-004
49 2.11055276E-003   6.64915030E-004
50 2.41206030E-003   6.63044958E-004
51 2.71356784E-003   6.60927063E-004
52 3.01507538E-003   6.58561942E-004
53 3.31658291E-003   6.55950279E-004
54 3.61809045E-003   6.53092845E-004
55 3.91959799E-003   6.49990513E-004
56 4.22110553E-003   6.46644253E-004
57 4.52261307E-003   6.43055149E-004
58 4.82412060E-003   6.39224399E-004
59 5.12562814E-003   6.35153323E-004
60 5.42713568E-003   6.30843374E-004
61 5.72864322E-003   6.26296143E-004
62 6.03015075E-003   6.21513371E-004
63 6.33165829E-003   6.16496952E-004
64 6.63316583E-003   6.11248947E-004
65 6.93467337E-003   6.05771591E-004
66 7.23618090E-003   6.00067302E-004
67 7.53768844E-003   5.94138692E-004
68 7.83919598E-003   5.87988573E-004
69 8.14070352E-003   5.81619972E-004
70 8.44221106E-003   5.75036135E-004
71 8.74371859E-003   5.68240539E-004
72 9.04522613E-003   5.61236899E-004
73 9.34673367E-003   5.54029182E-004
74 9.64824121E-003   5.46621608E-004
75 9.94974874E-003   5.39018666E-004
76 1.02512563E-002   5.31225115E-004
77 1.05527638E-002   5.23245996E-004
78 1.08542714E-002   5.15086636E-004
79 1.11557789E-002   5.06752657E-004
80 1.14572864E-002   4.98249977E-004
81 1.17587940E-002   4.89584821E-004
82 1.20603015E-002   4.80763717E-004
83 1.23618090E-002   4.71793506E-004
84 1.26633166E-002   4.62681339E-004
85 1.29648241E-002   4.53434682E-004
86 1.32663317E-002   4.44061311E-004
87 1.35678392E-002   4.34569318E-004
88 1.38693467E-002   4.24967100E-004
89 1.41708543E-002   4.15263362E-004
90 1.44723618E-002   4.05467111E-004
91 1.47738693E-002   3.95587648E-004
92 1.50753769E-002   3.85634563E-004
93 1.53768844E-002   3.75617726E-004
94 1.56783920E-002   3.65547276E-004
95 1.59798995E-002   3.55433614E-004
96 1.62814070E-002   3.45287387E-004
97 1.65829146E-002   3.35119475E-004
```

```
98  1.68844221E-002   3.24940979E-004
99  1.71859296E-002   3.14763205E-004
100 1.74874372E-002   3.04597646E-004
101 1.77889447E-002   2.94455965E-004
102 1.80904523E-002   2.84349976E-004
103 1.83919598E-002   2.74291626E-004
104 1.86934673E-002   2.64292973E-004
105 1.89949749E-002   2.54366165E-004
106 1.92964824E-002   2.44523419E-004
107 1.95979899E-002   2.34776998E-004
108 1.98994975E-002   2.25139188E-004
109 2.02010050E-002   2.15622276E-004
110 2.05025126E-002   2.06238522E-004
111 2.08040201E-002   1.97000139E-004
112 2.11055276E-002   1.87919269E-004
113 2.14070352E-002   1.79007954E-004
114 2.17085427E-002   1.70278117E-004
115 2.20100503E-002   1.61741532E-004
116 2.23115578E-002   1.53409804E-004
117 2.26130653E-002   1.45294345E-004
118 2.29145729E-002   1.37406345E-004
119 2.32160804E-002   1.29756755E-004
120 2.35175879E-002   1.22356260E-004
121 2.38190955E-002   1.15215257E-004
122 2.41206030E-002   1.08343834E-004
123 2.44221106E-002   1.01751749E-004
124 2.47236181E-002   9.54484062E-005
125 2.50251256E-002   8.94428395E-005
126 2.53266332E-002   8.37436917E-005
127 2.56281407E-002   7.83591965E-005
128 2.59296482E-002   7.32971608E-005
129 2.62311558E-002   6.85649484E-005
130 2.65326633E-002   6.41694642E-005
131 2.68341709E-002   6.01171395E-005
132 2.71356784E-002   5.64139184E-005
133 2.74371859E-002   5.30652457E-005
134 2.77386935E-002   5.00760545E-005
135 2.80402010E-002   4.74507567E-005
136 2.83417085E-002   4.51932330E-005
137 2.86432161E-002   4.33068251E-005
138 2.89447236E-002   4.17943285E-005
139 2.92462312E-002   4.06579868E-005
140 2.95477387E-002   3.98994867E-005
141 2.98492462E-002   3.95199547E-005
142 3.01507538E-002   3.95199547E-005
143 3.04522613E-002   3.98994867E-005
144 3.07537688E-002   4.06579868E-005
145 3.10552764E-002   4.17943285E-005
146 3.13567839E-002   4.33068251E-005
147 3.16582915E-002   4.51932330E-005
```

```
148 3.19597990E-002   4.74507567E-005
149 3.22613065E-002   5.00760545E-005
150 3.25628141E-002   5.30652457E-005
151 3.28643216E-002   5.64139184E-005
152 3.31658291E-002   6.01171395E-005
153 3.34673367E-002   6.41694642E-005
154 3.37688442E-002   6.85649484E-005
155 3.40703518E-002   7.32971608E-005
156 3.43718593E-002   7.83591965E-005
157 3.46733668E-002   8.37436917E-005
158 3.49748744E-002   8.94428395E-005
159 3.52763819E-002   9.54484062E-005
160 3.55778894E-002   1.01751749E-004
161 3.58793970E-002   1.08343834E-004
162 3.61809045E-002   1.15215257E-004
163 3.64824121E-002   1.22356260E-004
164 3.67839196E-002   1.29756755E-004
165 3.70854271E-002   1.37406345E-004
166 3.73869347E-002   1.45294345E-004
167 3.76884422E-002   1.53409804E-004
168 3.79899497E-002   1.61741532E-004
169 3.82914573E-002   1.70278117E-004
170 3.85929648E-002   1.79007954E-004
171 3.88944724E-002   1.87919269E-004
172 3.91959799E-002   1.97000139E-004
173 3.94974874E-002   2.06238522E-004
174 3.97989950E-002   2.15622276E-004
175 4.01005025E-002   2.25139188E-004
176 4.04020101E-002   2.34776998E-004
177 4.07035176E-002   2.44523419E-004
178 4.10050251E-002   2.54366165E-004
179 4.13065327E-002   2.64292973E-004
180 4.16080402E-002   2.74291626E-004
181 4.19095477E-002   2.84349976E-004
182 4.22110553E-002   2.94455965E-004
183 4.25125628E-002   3.04597646E-004
184 4.28140704E-002   3.14763205E-004
185 4.31155779E-002   3.24940979E-004
186 4.34170854E-002   3.35119475E-004
187 4.37185930E-002   3.45287387E-004
188 4.40201005E-002   3.55433614E-004
189 4.43216080E-002   3.65547276E-004
190 4.46231156E-002   3.75617726E-004
191 4.49246231E-002   3.85634563E-004
192 4.52261307E-002   3.95587648E-004
193 4.55276382E-002   4.05467111E-004
194 4.58291457E-002   4.15263362E-004
195 4.61306533E-002   4.24967100E-004
196 4.64321608E-002   4.34569318E-004
197 4.67336683E-002   4.44061311E-004
```

```
198 4.70351759E-002   4.53434682E-004
199 4.73366834E-002   4.62681339E-004
200 4.76381910E-002   4.71793506E-004
201 4.79396985E-002   4.80763717E-004
202 4.82412060E-002   4.89584821E-004
203 4.85427136E-002   4.98249977E-004
204 4.88442211E-002   5.06752657E-004
205 4.91457286E-002   5.15086636E-004
206 4.94472362E-002   5.23245996E-004
207 4.97487437E-002   5.31225115E-004
208 5.00502513E-002   5.39018666E-004
209 5.03517588E-002   5.46621608E-004
210 5.06532663E-002   5.54029182E-004
211 5.09547739E-002   5.61236899E-004
212 5.12562814E-002   5.68240539E-004
213 5.15577889E-002   5.75036135E-004
214 5.18592965E-002   5.81619972E-004
215 5.21608040E-002   5.87988573E-004
216 5.24623116E-002   5.94138692E-004
217 5.27638191E-002   6.00067302E-004
218 5.30653266E-002   6.05771591E-004
219 5.33668342E-002   6.11248947E-004
220 5.36683417E-002   6.16496952E-004
221 5.39698492E-002   6.21513371E-004
222 5.42713568E-002   6.26296143E-004
223 5.45728643E-002   6.30843374E-004
224 5.48743719E-002   6.35153323E-004
225 5.51758794E-002   6.39224399E-004
226 5.54773869E-002   6.43055149E-004
227 5.57788945E-002   6.46644253E-004
228 5.60804020E-002   6.49990513E-004
229 5.63819095E-002   6.53092845E-004
230 5.66834171E-002   6.55950279E-004
231 5.69849246E-002   6.58561942E-004
232 5.72864322E-002   6.60927063E-004
233 5.75879397E-002   6.63044958E-004
234 5.78894472E-002   6.64915030E-004
235 5.81909548E-002   6.66536764E-004
236 5.84924623E-002   6.67909721E-004
237 5.87939698E-002   6.69033536E-004
238 5.90954774E-002   6.69907915E-004
239 5.93969849E-002   6.70532631E-004
240 5.96984925E-002   6.70907525E-004
241 6.00000000E-002   6.71032500E-004
242   </V_PROFILE>
243
244 </BATCH>
```

C. Summary of Numerical Results

The engine speed N is given in rpm, mole numbers n are given in mol and production rates $\dot{n}$ are given in mol s^{-1}. The subscript numbers denote the exponent.

C.1. Simplified Dry Air

ϕ	N	n_{H_2}	n_{CO}	S_{H_2}	S_{H_2O}	S_{CO}	S_{CO_2}	X_{fuel}	$\dot{n}_{H_2}$	$\dot{n}_{CO}$	$\dot{n}_{syngas}$
1.5	250	1.443_{-3}	1.326_{-3}	3.521_{-1}	6.477_{-1}	6.297_{-1}	3.703_{-1}	1.000_{0}	3.006_{-3}	2.763_{-3}	5.769_{-3}
1.5	500	1.434_{-3}	1.335_{-3}	3.499_{-1}	6.498_{-1}	6.338_{-1}	3.662_{-1}	1.000_{0}	5.975_{-3}	5.561_{-3}	1.154_{-2}
1.5	1,000	1.421_{-3}	1.347_{-3}	3.468_{-1}	6.528_{-1}	6.397_{-1}	3.603_{-1}	1.000_{0}	1.184_{-2}	1.123_{-2}	2.307_{-2}
1.5	1,500	1.413_{-3}	1.356_{-3}	3.447_{-1}	6.548_{-1}	6.437_{-1}	3.563_{-1}	1.000_{0}	1.766_{-2}	1.694_{-2}	3.460_{-2}
1.5	2,000	1.406_{-3}	1.362_{-3}	3.431_{-1}	6.564_{-1}	6.468_{-1}	3.532_{-1}	1.000_{0}	2.343_{-2}	2.270_{-2}	4.613_{-2}
1.5	2,500	1.401_{-3}	1.367_{-3}	3.418_{-1}	6.577_{-1}	6.493_{-1}	3.507_{-1}	1.000_{0}	2.918_{-2}	2.848_{-2}	5.766_{-2}
1.5	3,000	1.396_{-3}	1.372_{-3}	3.407_{-1}	6.587_{-1}	6.514_{-1}	3.486_{-1}	1.000_{0}	3.490_{-2}	3.429_{-2}	6.920_{-2}
1.5	3,500	1.392_{-3}	1.375_{-3}	3.398_{-1}	6.596_{-1}	6.531_{-1}	3.468_{-1}	1.000_{0}	4.061_{-2}	4.012_{-2}	8.073_{-2}
2.0	250	3.090_{-3}	2.215_{-3}	5.905_{-1}	4.093_{-1}	8.234_{-1}	1.766_{-1}	1.000_{0}	6.439_{-3}	4.614_{-3}	1.105_{-2}
2.0	500	3.072_{-3}	2.233_{-3}	5.870_{-1}	4.127_{-1}	8.301_{-1}	1.699_{-1}	1.000_{0}	1.280_{-2}	9.303_{-3}	2.210_{-2}
2.0	1,000	3.055_{-3}	2.250_{-3}	5.837_{-1}	4.160_{-1}	8.364_{-1}	1.635_{-1}	1.000_{0}	2.546_{-2}	1.875_{-2}	4.420_{-2}
2.0	1,500	3.045_{-3}	2.259_{-3}	5.818_{-1}	4.178_{-1}	8.399_{-1}	1.600_{-1}	1.000_{0}	3.806_{-2}	2.824_{-2}	6.630_{-2}
2.0	2,000	3.039_{-3}	2.266_{-3}	5.806_{-1}	4.190_{-1}	8.423_{-1}	1.576_{-1}	1.000_{0}	5.064_{-2}	3.776_{-2}	8.840_{-2}
2.0	2,500	3.034_{-3}	2.270_{-3}	5.796_{-1}	4.199_{-1}	8.441_{-1}	1.558_{-1}	1.000_{0}	6.320_{-2}	4.730_{-2}	1.105_{-1}
2.0	3,000	3.030_{-3}	2.274_{-3}	5.789_{-1}	4.207_{-1}	8.455_{-1}	1.545_{-1}	1.000_{0}	7.574_{-2}	5.685_{-2}	1.326_{-1}

ϕ	N	n_{H_2}	n_{CO}	S_{H_2}	S_{H_2O}	S_{CO}	S_{CO_2}	X_{fuel}	$\dot{n}_{H_2}$	$\dot{n}_{CO}$	$\dot{n}_{syngas}$
2.0	3,500	3.026_{-3}	2.277_{-3}	5.782_{-1}	4.212_{-1}	8.465_{-1}	1.534_{-1}	1.000_{0}	8.827_{-2}	6.641_{-2}	1.547_{-1}
2.5	250	4.697_{-3}	2.939_{-3}	7.481_{-1}	2.516_{-1}	9.110_{-1}	8.895_{-2}	1.000_{0}	9.785_{-3}	6.123_{-3}	1.591_{-2}
2.5	500	4.685_{-3}	2.952_{-3}	7.462_{-1}	2.535_{-1}	9.148_{-1}	8.510_{-2}	1.000_{0}	1.952_{-2}	1.230_{-2}	3.182_{-2}
2.5	1,000	4.673_{-3}	2.963_{-3}	7.444_{-1}	2.554_{-1}	9.184_{-1}	8.152_{-2}	1.000_{0}	3.894_{-2}	2.469_{-2}	6.364_{-2}
2.5	1,500	4.658_{-3}	2.969_{-3}	7.425_{-1}	2.573_{-1}	9.209_{-1}	7.895_{-2}	9.993_{-1}	5.822_{-2}	3.712_{-2}	9.534_{-2}
2.5	2,000	4.587_{-3}	2.946_{-3}	7.357_{-1}	2.634_{-1}	9.193_{-1}	7.866_{-2}	9.930_{-1}	7.646_{-2}	4.910_{-2}	1.256_{-1}
2.5	2,500	4.430_{-3}	2.868_{-3}	7.187_{-1}	2.767_{-1}	9.052_{-1}	8.181_{-2}	9.813_{-1}	9.229_{-2}	5.976_{-2}	1.520_{-1}
2.5	3,000	4.181_{-3}	2.726_{-3}	6.874_{-1}	2.988_{-1}	8.715_{-1}	8.769_{-2}	9.681_{-1}	1.045_{-1}	6.816_{-2}	1.727_{-1}
2.5	3,500	3.806_{-3}	2.485_{-3}	6.339_{-1}	3.344_{-1}	8.045_{-1}	9.705_{-2}	9.553_{-1}	1.110_{-1}	7.248_{-2}	1.835_{-1}
3.0	250	6.092_{-3}	3.509_{-3}	8.523_{-1}	1.476_{-1}	9.548_{-1}	4.504_{-2}	9.867_{-1}	1.269_{-2}	7.310_{-3}	2.000_{-2}
3.0	500	5.592_{-3}	3.304_{-3}	8.192_{-1}	1.781_{-1}	9.403_{-1}	5.339_{-2}	9.412_{-1}	2.330_{-2}	1.377_{-2}	3.707_{-2}
3.0	1,000	4.739_{-3}	2.880_{-3}	7.357_{-1}	2.401_{-1}	8.678_{-1}	7.059_{-2}	8.869_{-1}	3.949_{-2}	2.400_{-2}	6.349_{-2}
3.0	1,500	4.133_{-3}	2.508_{-3}	6.532_{-1}	2.919_{-1}	7.692_{-1}	8.269_{-2}	8.710_{-1}	5.166_{-2}	3.136_{-2}	8.302_{-2}
3.0	2,000	3.674_{-3}	2.185_{-3}	5.804_{-1}	3.349_{-1}	6.699_{-1}	9.034_{-2}	8.714_{-1}	6.123_{-2}	3.642_{-2}	9.766_{-2}
3.0	2,500	3.304_{-3}	1.898_{-3}	5.172_{-1}	3.716_{-1}	5.767_{-1}	9.456_{-2}	8.795_{-1}	6.883_{-2}	3.955_{-2}	1.084_{-1}
3.0	3,000	4.640_{-5}	1.086_{-4}	7.833_{-2}	5.252_{-1}	3.382_{-1}	7.350_{-3}	7.694_{-2}	1.159_{-3}	2.715_{-3}	3.874_{-3}
3.0	3,500	7.960_{-6}	1.230_{-5}	5.482_{-2}	4.482_{-1}	1.531_{-1}	1.281_{-3}	1.848_{-2}	2.321_{-4}	3.577_{-4}	5.898_{-4}
3.5	250	5.322_{-3}	3.127_{-3}	8.067_{-1}	1.817_{-1}	9.172_{-1}	5.672_{-2}	8.066_{-1}	1.109_{-2}	6.514_{-3}	1.760_{-2}
3.5	500	4.354_{-3}	2.606_{-3}	6.943_{-1}	2.562_{-1}	8.039_{-1}	7.695_{-2}	7.662_{-1}	1.814_{-2}	1.086_{-2}	2.900_{-2}
3.5	1,000	3.522_{-3}	2.034_{-3}	5.582_{-1}	3.320_{-1}	6.236_{-1}	8.947_{-2}	7.712_{-1}	2.935_{-2}	1.695_{-2}	4.630_{-2}
3.5	1,500	3.190_{-3}	1.754_{-3}	4.942_{-1}	3.654_{-1}	5.258_{-1}	8.984_{-2}	7.895_{-1}	3.988_{-2}	2.192_{-2}	6.180_{-2}
3.5	2,000	3.030_{-3}	1.606_{-3}	4.619_{-1}	3.844_{-1}	4.742_{-1}	8.624_{-2}	8.021_{-1}	5.049_{-2}	2.677_{-2}	7.727_{-2}
3.5	2,500	1.250_{-5}	2.180_{-5}	5.844_{-2}	4.574_{-1}	1.850_{-1}	1.908_{-3}	2.421_{-2}	2.601_{-4}	4.547_{-4}	7.149_{-4}
3.5	3,000	4.930_{-6}	6.160_{-6}	5.058_{-2}	4.234_{-1}	1.128_{-1}	6.660_{-4}	1.088_{-2}	1.234_{-4}	1.539_{-4}	2.772_{-4}
3.5	3,500	2.950_{-6}	2.900_{-6}	4.727_{-2}	4.069_{-1}	8.239_{-2}	3.550_{-4}	6.902_{-3}	8.614_{-5}	8.454_{-5}	1.707_{-4}
4.0	250	4.102_{-3}	2.448_{-3}	6.775_{-1}	2.615_{-1}	7.792_{-1}	8.140_{-2}	6.688_{-1}	8.546_{-3}	5.100_{-3}	1.365_{-2}
4.0	500	3.383_{-3}	1.947_{-3}	5.507_{-1}	3.279_{-1}	6.114_{-1}	9.118_{-2}	6.791_{-1}	1.409_{-2}	8.113_{-3}	2.221_{-2}
4.0	1,000	3.006_{-3}	1.611_{-3}	4.698_{-1}	3.666_{-1}	4.860_{-1}	8.820_{-2}	7.083_{-1}	2.505_{-2}	1.342_{-2}	3.848_{-2}

ϕ	N	n_{H_2}	n_{CO}	S_{H_2}	S_{H_2O}	S_{CO}	S_{CO_2}	X_{fuel}	$\dot{n}_{H_2}$	$\dot{n}_{CO}$	$\dot{n}_{syngas}$
4.0	1,500	2.920_{-3}	1.522_{-3}	4.470_{-1}	3.799_{-1}	4.499_{-1}	7.958_{-2}	7.230_{-1}	3.650_{-2}	1.903_{-2}	5.552_{-2}
4.0	2,000	1.170_{-5}	1.970_{-5}	5.716_{-2}	4.479_{-1}	1.738_{-1}	1.650_{-3}	2.086_{-2}	1.946_{-4}	3.286_{-4}	5.233_{-4}
4.0	2,500	4.180_{-6}	4.740_{-6}	4.891_{-2}	4.110_{-1}	9.845_{-2}	4.960_{-4}	8.565_{-3}	8.711_{-5}	9.883_{-5}	1.859_{-4}
4.0	3,000	2.400_{-6}	2.060_{-6}	4.561_{-2}	3.937_{-1}	6.885_{-2}	2.460_{-4}	5.225_{-3}	6.012_{-5}	5.159_{-5}	1.117_{-4}
4.0	3,500	1.610_{-6}	1.100_{-6}	4.356_{-2}	3.824_{-1}	5.197_{-2}	1.480_{-4}	3.640_{-3}	4.704_{-5}	3.209_{-5}	7.913_{-5}
4.5	250	3.291_{-3}	1.913_{-3}	5.568_{-1}	3.206_{-1}	6.221_{-1}	9.375_{-2}	5.995_{-1}	6.856_{-3}	3.986_{-3}	1.084_{-2}
4.5	500	2.924_{-3}	1.597_{-3}	4.749_{-1}	3.575_{-1}	4.989_{-1}	9.156_{-2}	6.253_{-1}	1.218_{-2}	6.653_{-3}	1.884_{-2}
4.5	1,000	2.817_{-3}	1.464_{-3}	4.390_{-1}	3.729_{-1}	4.394_{-1}	7.907_{-2}	6.523_{-1}	2.348_{-2}	1.220_{-2}	3.568_{-2}
4.5	1,500	2.740_{-5}	5.660_{-5}	6.703_{-2}	4.767_{-1}	2.513_{-1}	3.695_{-3}	3.872_{-2}	3.421_{-4}	7.075_{-4}	1.050_{-3}
4.5	2,000	4.480_{-6}	5.170_{-6}	4.886_{-2}	4.072_{-1}	9.950_{-2}	4.990_{-4}	8.423_{-3}	7.473_{-5}	8.613_{-5}	1.609_{-4}
4.5	2,500	2.280_{-6}	1.860_{-6}	4.487_{-2}	3.860_{-1}	6.395_{-2}	2.090_{-4}	4.607_{-3}	4.759_{-5}	3.879_{-5}	8.638_{-5}
4.5	3,000	1.440_{-6}	8.900_{-7}	4.257_{-2}	3.729_{-1}	4.575_{-2}	1.140_{-4}	3.025_{-3}	3.593_{-5}	2.224_{-5}	5.817_{-5}
4.5	3,500	9.960_{-7}	4.880_{-7}	4.093_{-2}	3.631_{-1}	3.458_{-2}	7.300_{-5}	2.165_{-3}	2.906_{-5}	1.422_{-5}	4.328_{-5}

C.2. Argon Gas Mixture

ϕ	N	n_{H_2}	n_{CO}	S_{H_2}	S_{H_2O}	S_{CO}	S_{CO_2}	X_{fuel}	$\dot{n}_{H_2}$	$\dot{n}_{CO}$	$\dot{n}_{syngas}$
1.5	250	1.355_{-3}	1.415_{-3}	3.305_{-1}	6.692_{-1}	6.717_{-1}	3.283_{-1}	1.000_{0}	2.822_{-3}	2.947_{-3}	5.769_{-3}
1.5	500	1.370_{-3}	1.399_{-3}	3.344_{-1}	6.654_{-1}	6.642_{-1}	3.358_{-1}	1.000_{0}	5.710_{-3}	5.828_{-3}	1.154_{-2}
1.5	1,000	1.383_{-3}	1.386_{-3}	3.375_{-1}	6.624_{-1}	6.584_{-1}	3.416_{-1}	1.000_{0}	1.152_{-2}	1.155_{-2}	2.308_{-2}
1.5	1,500	1.387_{-3}	1.383_{-3}	3.384_{-1}	6.614_{-1}	6.565_{-1}	3.435_{-1}	1.000_{0}	1.733_{-2}	1.728_{-2}	3.462_{-2}
1.5	2,000	1.388_{-3}	1.381_{-3}	3.387_{-1}	6.610_{-1}	6.559_{-1}	3.441_{-1}	1.000_{0}	2.314_{-2}	2.302_{-2}	4.615_{-2}
1.5	2,500	1.388_{-3}	1.381_{-3}	3.388_{-1}	6.610_{-1}	6.557_{-1}	3.443_{-1}	1.000_{0}	2.892_{-2}	2.877_{-2}	5.769_{-2}
1.5	3,000	1.388_{-3}	1.381_{-3}	3.388_{-1}	6.610_{-1}	6.558_{-1}	3.442_{-1}	1.000_{0}	3.470_{-2}	3.453_{-2}	6.923_{-2}
1.5	3,500	1.388_{-3}	1.382_{-3}	3.387_{-1}	6.611_{-1}	6.561_{-1}	3.439_{-1}	1.000_{0}	4.048_{-2}	4.030_{-2}	8.077_{-2}
2.0	250	3.097_{-3}	2.209_{-3}	5.918_{-1}	4.082_{-1}	8.213_{-1}	1.787_{-1}	1.000_{0}	6.453_{-3}	4.602_{-3}	1.106_{-2}
2.0	500	3.081_{-3}	2.225_{-3}	5.888_{-1}	4.112_{-1}	8.272_{-1}	1.728_{-1}	1.000_{0}	1.284_{-2}	9.271_{-3}	2.211_{-2}
2.0	1,000	3.065_{-3}	2.241_{-3}	5.857_{-1}	4.143_{-1}	8.332_{-1}	1.668_{-1}	1.000_{0}	2.555_{-2}	1.867_{-2}	4.422_{-2}
2.0	1,500	3.056_{-3}	2.250_{-3}	5.839_{-1}	4.160_{-1}	8.366_{-1}	1.634_{-1}	1.000_{0}	3.820_{-2}	2.813_{-2}	6.633_{-2}
2.0	2,000	3.050_{-3}	2.257_{-3}	5.827_{-1}	4.173_{-1}	8.390_{-1}	1.610_{-1}	1.000_{0}	5.083_{-2}	3.761_{-2}	8.844_{-2}
2.0	2,500	3.045_{-3}	2.262_{-3}	5.817_{-1}	4.182_{-1}	8.409_{-1}	1.591_{-1}	1.000_{0}	6.343_{-2}	4.712_{-2}	1.105_{-1}
2.0	3,000	3.041_{-3}	2.266_{-3}	5.809_{-1}	4.190_{-1}	8.424_{-1}	1.576_{-1}	1.000_{0}	7.601_{-2}	5.664_{-2}	1.327_{-1}
2.0	3,500	3.037_{-3}	2.269_{-3}	5.803_{-1}	4.196_{-1}	8.436_{-1}	1.564_{-1}	1.000_{0}	8.858_{-2}	6.618_{-2}	1.548_{-1}
2.5	250	4.700_{-3}	2.939_{-3}	7.486_{-1}	2.514_{-1}	9.109_{-1}	8.911_{-2}	1.000_{0}	9.791_{-3}	6.123_{-3}	1.591_{-2}
2.5	500	4.687_{-3}	2.952_{-3}	7.465_{-1}	2.535_{-1}	9.148_{-1}	8.516_{-2}	1.000_{0}	1.953_{-2}	1.230_{-2}	3.183_{-2}
2.5	1,000	4.675_{-3}	2.963_{-3}	7.446_{-1}	2.554_{-1}	9.185_{-1}	8.148_{-2}	1.000_{0}	3.896_{-2}	2.470_{-2}	6.365_{-2}
2.5	1,500	4.668_{-3}	2.970_{-3}	7.436_{-1}	2.564_{-1}	9.206_{-1}	7.944_{-2}	1.000_{0}	5.835_{-2}	3.713_{-2}	9.548_{-2}
2.5	2,000	4.664_{-3}	2.975_{-3}	7.429_{-1}	2.571_{-1}	9.220_{-1}	7.803_{-2}	1.000_{0}	7.773_{-2}	4.958_{-2}	1.273_{-1}
2.5	2,500	4.660_{-3}	2.978_{-3}	7.423_{-1}	2.577_{-1}	9.230_{-1}	7.697_{-2}	1.000_{0}	9.709_{-2}	6.204_{-2}	1.591_{-1}
2.5	3,000	4.658_{-3}	2.981_{-3}	7.419_{-1}	2.581_{-1}	9.239_{-1}	7.612_{-2}	1.000_{0}	1.164_{-1}	7.452_{-2}	1.910_{-1}
2.5	3,500	4.655_{-3}	2.983_{-3}	7.415_{-1}	2.585_{-1}	9.246_{-1}	7.542_{-2}	1.000_{0}	1.358_{-1}	8.701_{-2}	2.228_{-1}
3.0	250	6.224_{-3}	3.565_{-3}	8.595_{-1}	1.405_{-1}	9.581_{-1}	4.194_{-2}	1.000_{0}	1.297_{-2}	7.428_{-3}	2.039_{-2}
3.0	500	6.216_{-3}	3.573_{-3}	8.585_{-1}	1.415_{-1}	9.601_{-1}	3.990_{-2}	1.000_{0}	2.590_{-2}	1.489_{-2}	4.079_{-2}

ϕ	N	n_{H_2}	n_{CO}	S_{H_2}	S_{H_2O}	S_{CO}	S_{CO_2}	X_{fuel}	$\dot{n}_{H_2}$	$\dot{n}_{CO}$	$\dot{n}_{syngas}$
3.0	1,000	6.209_{-3}	3.580_{-3}	8.575_{-1}	1.425_{-1}	9.620_{-1}	3.800_{-2}	1.000_{0}	5.174_{-2}	2.983_{-2}	8.158_{-2}
3.0	1,500	6.205_{-3}	3.584_{-3}	8.569_{-1}	1.431_{-1}	9.631_{-1}	3.694_{-2}	1.000_{0}	7.757_{-2}	4.480_{-2}	1.224_{-1}
3.0	2,000	6.203_{-3}	3.587_{-3}	8.566_{-1}	1.434_{-1}	9.638_{-1}	3.622_{-2}	1.000_{0}	1.034_{-1}	5.978_{-2}	1.632_{-1}
3.0	2,500	6.201_{-3}	3.589_{-3}	8.563_{-1}	1.437_{-1}	9.643_{-1}	3.568_{-2}	1.000_{0}	1.292_{-1}	7.476_{-2}	2.039_{-1}
3.0	3,000	6.199_{-3}	3.590_{-3}	8.561_{-1}	1.439_{-1}	9.648_{-1}	3.524_{-2}	1.000_{0}	1.550_{-1}	8.975_{-2}	2.447_{-1}
3.0	3,500	6.197_{-3}	3.591_{-3}	8.558_{-1}	1.442_{-1}	9.651_{-1}	3.486_{-2}	9.999_{-1}	1.807_{-1}	1.048_{-1}	2.855_{-1}
3.5	250	7.651_{-3}	4.122_{-3}	9.412_{-1}	5.882_{-2}	9.866_{-1}	1.341_{-2}	9.996_{-1}	1.594_{-2}	8.587_{-3}	2.453_{-2}
3.5	500	7.516_{-3}	4.073_{-3}	9.350_{-1}	6.490_{-2}	9.856_{-1}	1.419_{-2}	9.881_{-1}	3.132_{-2}	1.697_{-2}	4.829_{-2}
3.5	1,000	7.010_{-3}	3.863_{-3}	9.079_{-1}	8.909_{-2}	9.725_{-1}	2.023_{-2}	9.480_{-1}	5.841_{-2}	3.219_{-2}	9.061_{-2}
3.5	1,500	6.560_{-3}	3.653_{-3}	8.754_{-1}	1.140_{-1}	9.468_{-1}	2.647_{-2}	9.197_{-1}	8.200_{-2}	4.566_{-2}	1.277_{-1}
3.5	2,000	6.195_{-3}	3.462_{-3}	8.422_{-1}	1.370_{-1}	9.140_{-1}	3.195_{-2}	9.023_{-1}	1.032_{-1}	5.771_{-2}	1.610_{-1}
3.5	2,500	5.893_{-3}	3.291_{-3}	8.104_{-1}	1.577_{-1}	8.786_{-1}	3.663_{-2}	8.918_{-1}	1.228_{-1}	6.856_{-2}	1.913_{-1}
3.5	3,000	5.638_{-3}	3.136_{-3}	7.808_{-1}	1.764_{-1}	8.430_{-1}	4.059_{-2}	8.856_{-1}	1.410_{-1}	7.841_{-2}	2.194_{-1}
3.5	3,500	5.420_{-3}	2.997_{-3}	7.535_{-1}	1.932_{-1}	8.086_{-1}	4.394_{-2}	8.820_{-1}	1.581_{-1}	8.741_{-2}	2.455_{-1}
4.0	250	7.221_{-3}	3.914_{-3}	9.315_{-1}	6.560_{-2}	9.787_{-1}	1.499_{-2}	8.616_{-1}	1.504_{-2}	8.154_{-3}	2.320_{-2}
4.0	500	6.322_{-3}	3.504_{-3}	8.698_{-1}	1.136_{-1}	9.331_{-1}	2.836_{-2}	8.069_{-1}	2.634_{-2}	1.460_{-2}	4.094_{-2}
4.0	1,000	5.338_{-3}	2.954_{-3}	7.633_{-1}	1.810_{-1}	8.174_{-1}	4.465_{-2}	7.760_{-1}	4.449_{-2}	2.462_{-2}	6.910_{-2}
4.0	1,500	4.804_{-3}	2.597_{-3}	6.879_{-1}	2.241_{-1}	7.196_{-1}	5.268_{-2}	7.750_{-1}	6.006_{-2}	3.246_{-2}	9.251_{-2}
4.0	2,000	4.474_{-3}	2.352_{-3}	6.362_{-1}	2.529_{-1}	6.475_{-1}	5.662_{-2}	7.805_{-1}	7.456_{-2}	3.920_{-2}	1.138_{-1}
4.0	2,500	4.254_{-3}	2.179_{-3}	6.000_{-1}	2.729_{-1}	5.949_{-1}	5.850_{-2}	7.871_{-1}	8.862_{-2}	4.539_{-2}	1.340_{-1}
4.0	3,000	4.101_{-3}	2.051_{-3}	5.740_{-1}	2.873_{-1}	5.559_{-1}	5.931_{-2}	7.933_{-1}	1.025_{-1}	5.129_{-2}	1.538_{-1}
4.0	3,500	3.991_{-3}	1.956_{-3}	5.548_{-1}	2.980_{-1}	5.265_{-1}	5.956_{-2}	7.989_{-1}	1.164_{-1}	5.704_{-2}	1.734_{-1}
4.5	250	5.762_{-3}	3.219_{-3}	8.407_{-1}	1.329_{-1}	9.059_{-1}	3.575_{-2}	6.977_{-1}	1.200_{-2}	6.707_{-3}	1.871_{-2}
4.5	500	4.803_{-3}	2.658_{-3}	7.204_{-1}	2.042_{-1}	7.691_{-1}	5.277_{-2}	6.787_{-1}	2.001_{-2}	1.108_{-2}	3.109_{-2}
4.5	1,000	4.065_{-3}	2.119_{-3}	5.976_{-1}	2.690_{-1}	6.013_{-1}	6.175_{-2}	6.931_{-1}	3.388_{-2}	1.766_{-2}	5.154_{-2}
4.5	1,500	3.789_{-3}	1.879_{-3}	5.453_{-1}	2.959_{-1}	5.222_{-1}	6.247_{-2}	7.084_{-1}	4.736_{-2}	2.349_{-2}	7.085_{-2}
4.5	2,000	3.661_{-3}	1.752_{-3}	5.188_{-1}	3.093_{-1}	4.795_{-1}	6.166_{-2}	7.196_{-1}	6.101_{-2}	2.919_{-2}	9.021_{-2}
4.5	2,500	3.596_{-3}	1.676_{-3}	5.038_{-1}	3.169_{-1}	4.539_{-1}	6.040_{-2}	7.280_{-1}	7.491_{-2}	3.492_{-2}	1.098_{-1}

ϕ	N	n_{H_2}	n_{CO}	S_{H_2}	S_{H_2O}	S_{CO}	S_{CO_2}	X_{fuel}	$\dot{n}_{H_2}$	$\dot{n}_{CO}$	$\dot{n}_{syngas}$
4.5	3,000	3.560_{-3}	1.629_{-3}	4.945_{-1}	3.217_{-1}	4.373_{-1}	5.890_{-2}	7.344_{-1}	8.900_{-2}	4.073_{-2}	1.297_{-1}
4.5	3,500	3.538_{-3}	1.598_{-3}	4.885_{-1}	3.253_{-1}	4.265_{-1}	5.732_{-2}	7.390_{-1}	1.032_{-1}	4.662_{-2}	1.498_{-1}

Bibliography

[1] G. P. Merker, C. Schwarz, *Grundlagen Verbrennungsmotoren*, (Ed.: R. Teichmann), Vieweg+Teubner Verlag, **2012**.

[2] B. Atakan, C. Schulz, S. Kaiser, T. Kasper, M. Fikri, U. Maas, O. Deutschmann, R. Schießl, Multifunktionale Stoff- und Energiewandlung, DFG Antrag, Forschergruppe 1993, **Dec. 2012**.

[3] J. B. Heywood, *Internal Combustion Engine Fundamentals*, McGraw-Hill New York, **1988**.

[4] H. L. Needleman, *Environmental Research* **2000**, *84*, 20–35.

[5] S. Fiveland, R. Agama, M. Christensen, B. Johansson, J. Hiltner, F. Maus, D. Assanis, *SAE Technical Paper* **2001**.

[6] M. I. Najafabadi, N. A. Aziz, *Journal of Combustion* **2013**, *2013*.

[7] J. H. Mack, S. M. Aceves, R. W. Dibble, *Energy* **2009**, *34*, 782–787.

[8] L. Von Szeszich, *Chemie Ingenieur Technik* **1956**, *28*, 190–195.

[9] M. H. McMillian, S. A. Lawson, *International Journal of Hydrogen Energy* **2006**, *31*, 847–860.

[10] G. A. Karim, I. Wierzba, *International Journal of Hydrogen Energy* **2008**, *33*, 2105–2110.

[11] Y. C. Yang, M. S. Lim, Y. N. Chun, *Fuel Processing Technology* **2009**, *90*, 553–557.

[12] M. H. Morsy, *International Journal of Hydrogen Energy* **2014**, *39*, 1096–1104.

[13] J. Warnatz, U. Maas, R. Dibble, *Combustion: Physical and Chemical Fundamentals, Modeling and Simulation, Experiments, Pollutant Formation*, Springer, **2006**.

[14] O. Deutschmann, S. Tischer, S. Kleditzsch, V. M. Janardhanan, C. Correa, D. Chatterjee, N. Mladenov, H. D. Minh, H. Karadeniz, DETCHEM Software package, **2013**, `www.detchem.com`.

[15] O. Deutschmann, F. Behrendt, J. Warnatz, *Catalysis Today* **1994**, *21*, 461–470.

[16] I. Chorkendorff, J. W. Niemantsverdriet, *Concepts of Modern Catalysis and Kinetics*, Wiley-VCH, Weinheim, 2nd ed., **2007**.

[17] A. Burcat in *Combustion Chemistry*, (Ed.: W. C. Gardiner, Jr), Springer, **1984**, pp. 455–473.

[18] B. J. McBride, S. Gordon, M. A. Reno, Coefficients for calculating thermodynamic and transport properties of individual species, tech. rep., NASA, **1993**.

[19] R. Ehrig, U. Nowak, LIMEX, **2000**, `www.zib.de`.

[20] G. Woschni, *SAE Technical Paper* **1967**.

[21] G. P. Smith, D. M. Golden, M. Frenklach, N. W. Moriarty, B. Eiteneer, M. Goldenberg, C. T. Bowman, R. K. Hanson, S. Song, W. C. Gardiner, Jr, V. V. Lissianski, Z. Qin, *GRI-Mech 3.0*, **July 1999**.

[22] H. J. Curran, *Preprints of Papers - American Chemical Society Division of Fuel Chemistry* **2004**, *49*, 263.

[23] J. M. Wallace, P. V. Hobbs, *Atmospheric Science: An Introductory Survey*, Academic Press, **2006**.

[24] J. Zhu, D. Zhang, K. King, *Fuel* **2001**, *80*, 899–905.

[25] R. Kee, F. Rupley, J. Miller, *The Chemkin Thermodynamic Database*, Sandia National Laboratories, **1990**.

[26] R. Kee, F. Rupley, J. Miller, *The Chemkin Thermodynamic Database*, Sandia National Laboratories, **1987**.

[27] J.-O. Olsson, P. Tunestal, B. Johansson, S. Fiveland, R. Agama, M. Willi, D. Assanis, *SAE Transactions* **2002**, *111*, 442–458.

[28] B. Lemke, C. Roodhouse, N. Glumac, H. Krier, *International Journal of Hydrogen Energy* **2005**, *30*, 893–902.

[29] F. Liu, J.-L. Consalvi, A. Fuentes, *Combustion and Flame* **2014**, DOI `http://dx.doi.org/10.1016/j.combustflame.2013.12.017`.

[30] S. B. Fiveland, D. N. Assanis, *SAE Technical Paper* **2000**.

[31] S. B. Fiveland, D. N. Assanis, *SAE Technical Paper* **2001**.